Investigating organic matter preservation through complexation with iron oxides in Lake Tantaré

Azadeh Joshani

A Thesis

in

The Department

of

Chemistry and Biochemistry

Presented in Partial Fulfillment of the Requirements

for the Degree of Master of Science (Chemistry) at

Concordia University

Montreal, Quebec, Canada

September 2015

CONCORDIA UNIVERSITY

School of graduate studies

This is to certify that the thesis prepared
By: Azadeh Joshani
Entitled: Investigating organic matter preservation through complexation with iron oxides in Lake Tantaré

and submitted in partial fulfillment of the requirements for the degree of

Master of Science (Chemistry)

complies with the regulations of the University and meets the accepted standards with respect to originality and quality.

Signed by the final Examining Committee:

______________________________ Chair
Dr. Guillaume Lamoureux
______________________________ Examiner
Dr. Christine DeWolf
______________________________ Examiner
Dr. Cameron Skinner
______________________________ Supervisor
Dr. Yves Gélinas
______________________________ Co-Supervisor

Approved by ____
Chair of Department or Graduate Program Director

__________________2015 ______________________________
Dean of Faculty

Abstract

Investigating organic matter preservation through complexation with iron oxides in Lake Tantaré

Azadeh Joshani

The biogeochemical cycles of iron (Fe) and organic carbon (OC) are closely interconnected. The concentration of reactive Fe is tightly controlled by soluble organic ligands in oceanic waters. In soils, Fe stabilizes OC by forming aggregates that shield OC from degradation. In sediments however; the role of Fe in the preservation of OC is only starting to be explored. To quantify the amount of OC retained in the solid phase through its interaction with Fe, an approach based on the reductive dissolution of reactive solid phase Fe, was applied. In this work, we investigated Fe-OC interactions in lake sediments, using sediments collected from Lake Tantaré, a system with two basins characterized by contrasting redox conditions in the summer. These contrasting redox conditions provided an opportunity to assess the importance of oxic/anoxic interfaces in the formation of stable OC-Fe complexes. We found 30.1 ± 6.4% of OC directly associated with Fe minerals. We characterized the Fe-associated and the non-Fe-associated OC pools at the elemental (OC, TN), isotopic ($\delta^{13}C$, $\delta^{15}N$) and functional group (FTIR) levels. We found large differences in OC:Fe and TN:Fe ratios among the two basins which were not related to differences in OM chemical composition but rather to differences in reactive iron concentrations stemming from the higher abundance of mackinawite (FeS). Since the affinity of OM for mackinawite is much lower than for iron hydroxides, using OC:Fe and TN:Fe ratios as a diagnostic tool for the type of OM-Fe interactions should be done with care in anoxic environment.

Acknowledgements

First and foremost I offer my sincerest gratitude to my supervisor, Dr. Yves Gélinas, who has supported me throughout my thesis with his patience and knowledge whilst allowing me the room to work in my own way. In all our meetings, I could feel his idealistic push at personal generosity, toward that which is the best. It was a pleasure and great honour to work with him.

I would like to give special thanks to Dr. Charles Gobeil for his support and guidance with respect to for his invaluable suggestions and guidance for my project. I would like also to thank my committee members Dr. Christine DeWolf and Dr. Cameron Skinner for their support throughout my master's research. The Geochemistry and Geodynamics Research Centre (GEOTOP) and Concordia University are also acknowledged.

In addition, I have been very privileged to get to know and to collaborate with many other great people who became friends over the last two years in Montreal. My appreciation also goes to my friends in the Concordia University, Amanda Gabriel, Andrew Barber, Kathryn Balind, Anja Moritz, Karine Lalonde.

Last but not the least, I would like to thank my husband and my friend, Peyman, who have supported me spiritually throughout writing this thesis.

Contribution of authors

Contributions from the different authors are addressed below. All analyses were carried out by Azadeh Joshani under the supervision of Dr. Yves Gélinas at Concordia University (elemental, isotopic and FTIR measurements). The samples were provided by Dr. Charles Gobeil from INRS-ETE. Andrew Barber, a Ph.D. student from the laboratory, contributed to this work through helpful discussions about the data presented in Chapter II. Kathryn Balind, a summer undergraduate student from the laboratory, helped with text editing (Chapters I and II). Dr. Gélinas and Gobeil provided inputs on a first version of the manuscript (Chapter II).

Table of Contents

List of figures

List of acronyms

AVS	Acid Volatile sulfide
Fe-OM	Iron associated Organic Matter
FTIR	Fourier Transform Infrared Spectroscopy
MUC-OM	Molecularly UnCharacterizable Organic Matter
OC	Organic Carbon
OC:Fe	Organic carbon to iron oxide molar ratio
OM	Organic Matter
TN	Total Nitrogen
TN:Fe	Total nitrogen to iron oxide molar ratio
δ	Difference of the stable isotope ratio of a sample versus that of a reference standard in per mil (‰)
$\delta^{13}C$	Stable carbon isotopic signature
$\delta^{15}N$	Stable Nitrogen isotopic signature
SWI	Sediment water interface
DCB	Dithionite Citrate Bicarbonate

1 General introduction

1.2 Carbon cycle

Since the beginning of the industrial revolution, human activities such as fossil fuel burning has been shifting the Earth's climate towards a new state.[2] The concentration of atmospheric carbon dioxide has increased with an unprecedented rate from a pre-Industrial value of 280 ppm to >400 ppm, as measured in April 2015 (NOAA). Based on ice core and geochemical proxy data this concentration is the highest yet.[2-5] Both the ocean and the terrestrial biosphere function as natural sinks of anthropogenic fossil fuel emissions and reduce the atmospheric carbon dioxide net accumulation to about half.[6] Through photosynthesis, atmospheric carbon dioxide (CO_2) is converted to organic matter (OM) that can be preserved in marine and lake sediments. Even though most OM is re-oxidized to inorganic carbon and eventually returns to the atmosphere, less than 1% of the yearly oceanic primary production of organic carbon (OC) becomes preserved in sediment for geological timescales.[7] While the preservation of this small OM fraction affects the atmospheric CO_2 and O_2 global cycles, the mechanisms of this OM preservation are still not clear.

Even though oceans are the major sink of carbon dioxide and largest pool of the Earth's carbon, inland freshwaters also are locations of intense carbon (C) cycling. Lakes and reservoirs cover about 1% of the Earth's surface, and because of this low surface coverage, inland waters are commonly considered to be a minor component of the carbon cycle. As a consequence, they are ignored in global estimates of carbon budget. However, recent studies[8,9] have demonstrated the substantial role of freshwater ecosystems in many key processes such as CO_2 production and OC storage. Lakes process large amounts of autochthonous (produced within the water body) and allochthonous (originating from external sources and imported in the water body) OC. One of the factors that explains the significant role of lakes in the global carbon budget is their high sedimentation rates that lead to high OC burial efficiencies. In comparison with marine environments, OC burial rates are generally 1-4 times higher in lakes and reservoirs.[10] Furthermore, OC burial rates have increased extensively in lakes due to land use changes by humans over the last few centuries (Figure 1-1).[11]

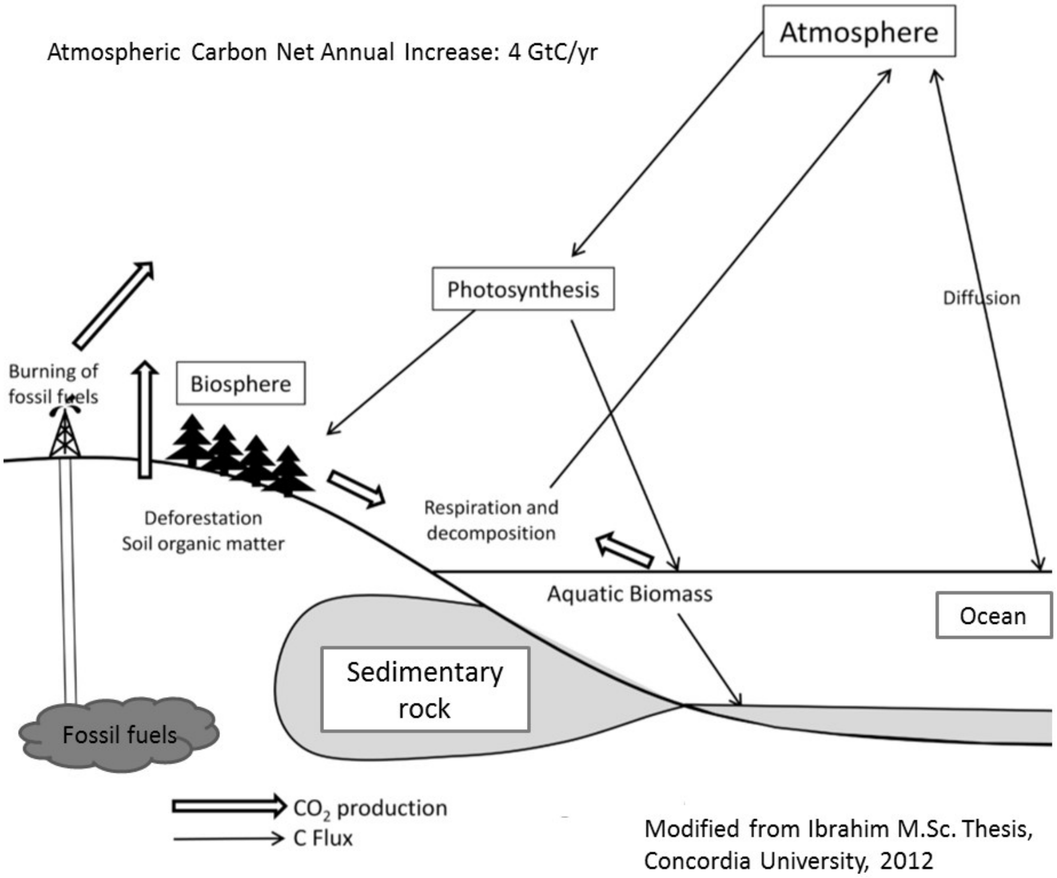

Figure 1-1: Simplified carbon cycle

1.3 Sediment composition

The major components of marine sediments are porewater, OM and eroded sand/clay particles that are subsequently transported by wind, water and ice or by gravity. These particles accumulate in layers in both coastal and deep ocean sediments. Porewater fills the space between the particles and makes up to 85% of sediment volume.[12] Organic matter is a minor component of the dry sediment (about 1 wt %), but is the most structurally complex constituent of the sediment matrix. OM can retain important molecular information such as, the origin of early living organisms or changes in redox conditions and temperature of the surface ocean.[13] Sedimentary material can be divided into three parts including: (i) an organic component: any carbon-made material derived from living or once-living organisms and their degradation products. The alteration products refer to any product that has been exposed to biophysicochemical processes such as chemical reactions, UV radiation or combustion; (ii) an inorganic component (e.g. mineral particles and metals), and (iii) a biogenic inorganic fraction (e.g. remains of plankton carbonate or opal shells). OM tends onto aggregate and sorb to mineral particles, resulting in the sinking of OM within the water column and accumulation of OM within surface sediments. Sedimentation occurs at different rates depending on several environmental parameters such as surface productivity, terrestrial inputs, and currents. In the deep ocean, the sedimentation rates vary between 0.1-1 cm yr^{-1}, however near river mouths and in coastal areas this rate varies over a broad range (1-20 cm yr^{-1}).[14]

Sediments cover 440,000,000 km^2 of the Earth's surface, with an average depth of 1.8 km.[15] By studying different layers of sediment deposited at different times, we are able to extract valuable information about the Earth's history and evolution as far back as 65 million years ago.[16]

1.4 Organic matter degradation

During the sinking of particles to the sea floor, the associated OM gets extensively (> 99%) yet selectively degraded, resulting in highly altered sedimentary records.[17] The first steps of OM alteration and degradation take place in the water column even before being integrated in the sediments, through biological and (photo)chemical processes such as respiration and photo oxidation. As shown in figure 1-2, only a small fraction of OM that is produced in the surface layer of the water column can escape degradation and eventually settle to the bottom of ocean.[13,18] Data collected from transmission electron microscopy (TEM) shows extreme changes in the structure of sinking organic-rich particles from surface to the seafloor.[19] OM from the surface is mostly composed of labile, high molecular weight biopolymers that are cleaved into less bioavailable polymers with low molecular weight (1-4 kDa), in the early stages of degradation.[18] Once in the sediment, these low molecular weight polymers and degradation products can remain in pore water as dissolved organic matter (DOM) or sorb to the surface of other particles.[20] Degradation processes are dynamic at the seafloor, and especially at the sediment water interface (SWI). Reduced OM molecules that have reached the SWI still have the potential to release energy, either through abiotic chemical oxidation or bacterial activity.

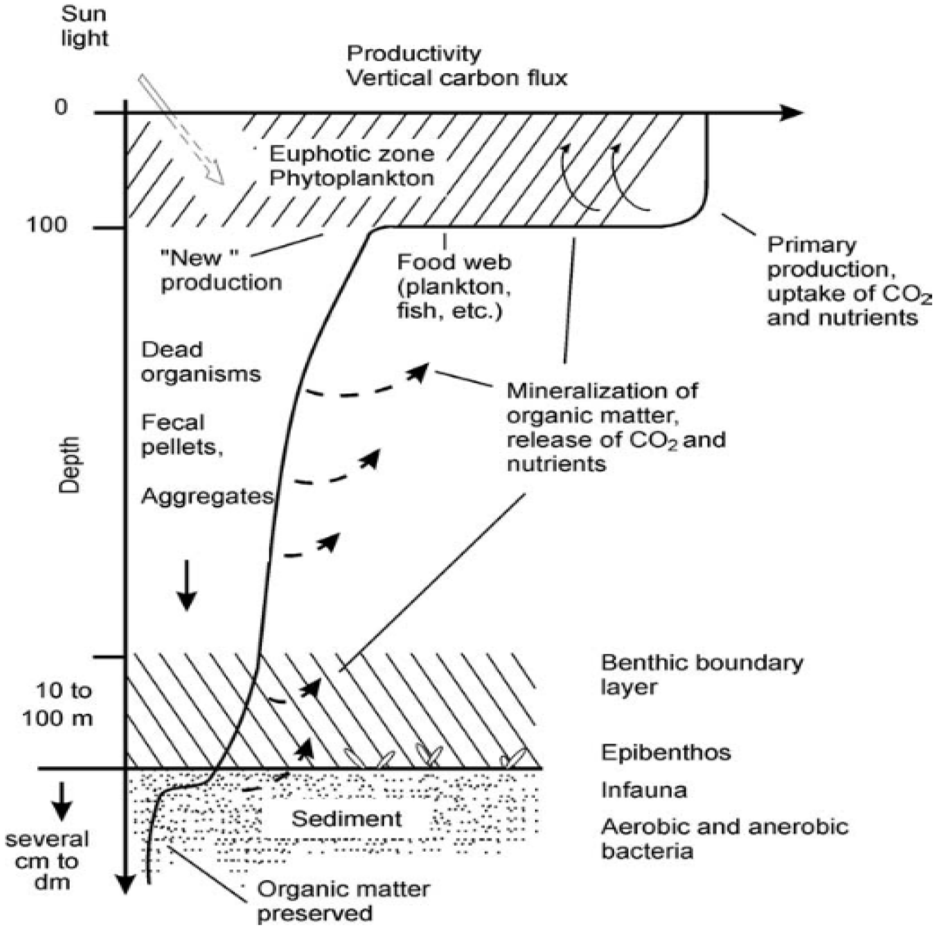

Figure 1-2: Schematic representation of OM flux to the ocean bottom. Recopied from ref. [17].

1.5 Organic matter preservation

Organic matter composition, bottom water oxygen content and OM production are three main factors that have been shown to control OC preservation.[21-23] The study of the effect of individual factors, without the effect of the others, is very difficult.[24-27]

Several proposed mechanisms responsible for OM preservation in sediment are (i) selective preservation (ii) geopolymerization (iii) physical protection. Different types of OM have different reactivities. Hedges and Keil (1995) were the first to use the expression "selective preservation" to explain the persistence of organic components accumulating in either oxic or anoxic sediments as the more biologically or chemically labile components are being degraded.[24]

Three main biochemical classes of organic compounds make up as much as 90% of marine algae biomass (e.g. carbohydrates, amino acid and lipids). However, because of chemical and biological alterations, as well as the selective preservation of recalcitrant macromolecular components, these labile compounds account only for a small fraction of total OM (less than ~10-20%) in sediments. The remaining fraction, labeled "Molecularly UnCharacterized Organic Matter (MUC-OM)", cannot be identified using conventional analytical techniques such as gas or liquid chromatography.[24] Lignin and algaenan, two types of biopolymers that exist in the cell wall of plants or algae, are two examples of the refractory molecules that are produced directly by autotrophs through photosynthesis process.[28]

In-situ condensation reactions or geopolymerization of smaller and more labile molecules can produce high molecular weight refractory molecules.[29] Melanoidins are one example of the recalcitrant high molecular weight heterogeneous polymers that are formed through the Maillard reaction of amino acids and sugars.[30] Other condensation reactions that probably occur in marine sediments include the sulfurization of lipids or carbohydrates[31], or the formation of heterocyclic N-containing molecules.[32] However due to the absence of direct evidence, the importance of this mechanism is still a subject of controversy.[24]

The most important mechanism of preservation is however physical protection, which occurs through interaction of OM with the biogenic components and inorganic sediment mineral matrix. This mechanism explains the presence of labile organic molecules in aged and highly re-worked marine sediments.[24] Strong organic-inorganic bonds inhibit enzymatic attack of the more labile organic molecules.[33] The reversible adsorption on the surface of minerals is the primary physical protection mechanism that is responsible for preservation of more than 90% of the OM in the sediments.[13] This association happens before its deposition on the SWI or during the early stages of burial in the sediment.

Finally, encapsulation of OM within the structure of biological inorganic material such as diatoms[34], or in mesopores (pores with diameters between 2 and 50 nm) of clay minerals[35] as well in the silicate sheet inter-layers of expandable clays (i.e. smectites) have been shown to protect OM, from even harsh chemical oxidants such as H_2O_2.[36] The relative importance of this mechanism compared to the other one still has to be assessed.

Lalonde et al. (2012) recently demonstrated the importance of physical protection through interaction with reducible metal oxides (i.e. iron and manganese) as an OM preservation mechanism. On average, they calculated that about 20% of organic compounds are associated to iron oxides in the world ocean. Earlier studies by Kaiser and Guggenberger (2000) reported that the association of redox-sensitive metal with OM occurs only in oxic soils. However, Lalonde et al. (2012) has shown that Fe-OM aggregates are metastable for thousands of years in marine sediment even under anoxic conditions. They proposed that the formation of co-precipitates of Fe-OM, due to the high affinity of Fe (III) for OM, increases stability and resistance to microbial degradation.

1.6 Interaction of iron with organic matter

The biogeochemical cycling of iron has significant effects on other redox-sensitive elements (i.e. carbon, nitrogen, sulfur, etc.) near the SWI, where electron transfer processes such as iron reduction or oxidation take place.[37] The affinity of iron for organic ligands (or vice versa) is also very strong (Fe-OM complexation constant is as high as 10^{12} M^{-1}) leading to the formation of strong bonds that protect OM from degradation, and ferric oxides from reduction.[38] The biogeochemical cycles of iron (Fe) and organic carbon (OC) are thus closely interconnected.[39] In soils, solid phase Fe stabilizes OC by forming mixed aggregates that shield OC and decrease its degradation rate.[40] On the other hand, it has been shown that OM controls the concentration of dissolved iron by increasing iron stability and bioavailability in different depositional environment such as sediment porewater,[41] oceanic water[42] and lakes.[43] Chemical/physical sorption of OM to iron oxides occurs through strong, predominantly covalent interactions between sedimentary OM and iron oxides through a ligand-exchange mechanism. In this association electronegative functional groups in OM (i.e. carboxyl or alcohol) replace hydroxyl groups of iron oxide particles.[44]

It has been proposed by Lalonde et al. (2012) that formation of Fe-OM aggregates takes place in oxic sediments where degradation of OM is more likely to happen.[45] In oxic surface sediment, nano-crystals of hydrated iron oxides (i.e. goethite) are thermodynamically stable.[46] Whereas in anoxic conditions, where Fe(III) reductively changes to soluble Fe(II), dissolved iron either diffuses upwards to the oxic region to form nano-particles and precipitate as Fe-OM, or diffuses downwards to precipitate as Fe-S (Figure 1-3). As long as the water column contains dissolved oxygen, iron will stay in the sediment due to fast oxidation of Fe(II) to Fe(III) and the low solubility of the Fe(III) nano-particle.[47]

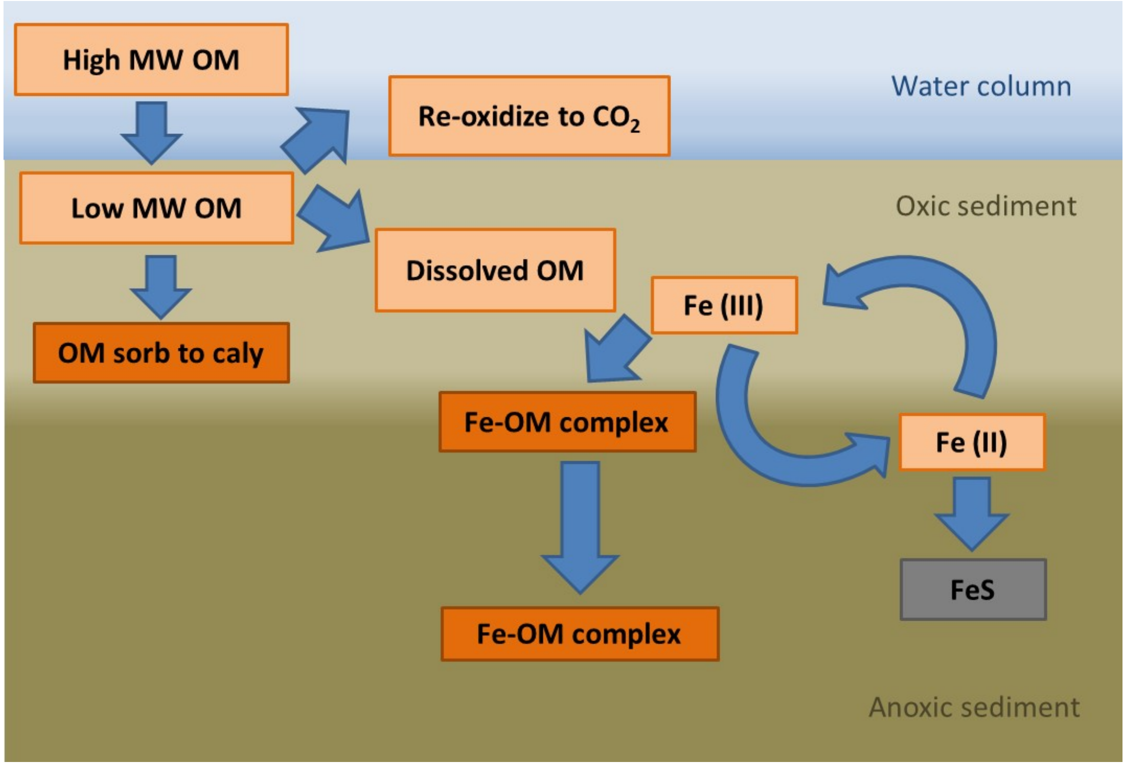

Figure 1-3: Iron and OM cycle in oxic/anoxic sediments and burial of Fe-OM in anoxic sediments (Modified from K. Lalonde Ph.D. thesis, Concordia University, 2014)

Iron thus acts as a shuttle, transferring OM from the oxic to the anoxic horizons in sediments where preservation is most likely happening.[48] In spite of having enough empirical data that support the role of iron in OM preservation, the exact mechanism of Fe and OM interaction is still not fully known.

1.7 Elemental and isotopic approach

Carbon, an important element in the atmosphere, the ocean and in living organisms, is constantly exchanged between the living and non-living reservoirs. The measurement of isotopic fractionation, enrichment of one isotope relative to another due to chemical or physical process, is a major diagnostic tool for determining diagenesis processes and the origin of the compound.

Stable isotope signatures of the sample ($\delta^{13}C_{sample}$) are calculated using the isotope ratio of a sample compared to that of an international standard. This ratio is expressed using the delta (δ) notation and is expressed in permil (‰) (Equation 1). The Pee Dee Belemnite (PDB) and atmospheric N_2 standards are the international reference standards for $\delta^{13}C$ and $\delta^{15}N$ analyses, respectively.

$$\delta^{13}C\ (\text{‰}) = \left(\frac{\left(\frac{^{13}C}{^{12}C}\right)_{sample}}{\left(\frac{^{13}C}{^{12}C}\right)_{reference}} - \frac{\left(\frac{^{13}C}{^{12}C}\right)_{reference}}{\left(\frac{^{13}C}{^{12}C}\right)_{reference}} \right) \times 1000 \qquad \text{Eq. 1}$$

Higher delta values (less negative) indicate increases in a sample's heavy isotope, relative to the standard, and lower values (or more negative) indicate that the sample is depleted in the heavier isotope compared to the standard (Figure 1-4).

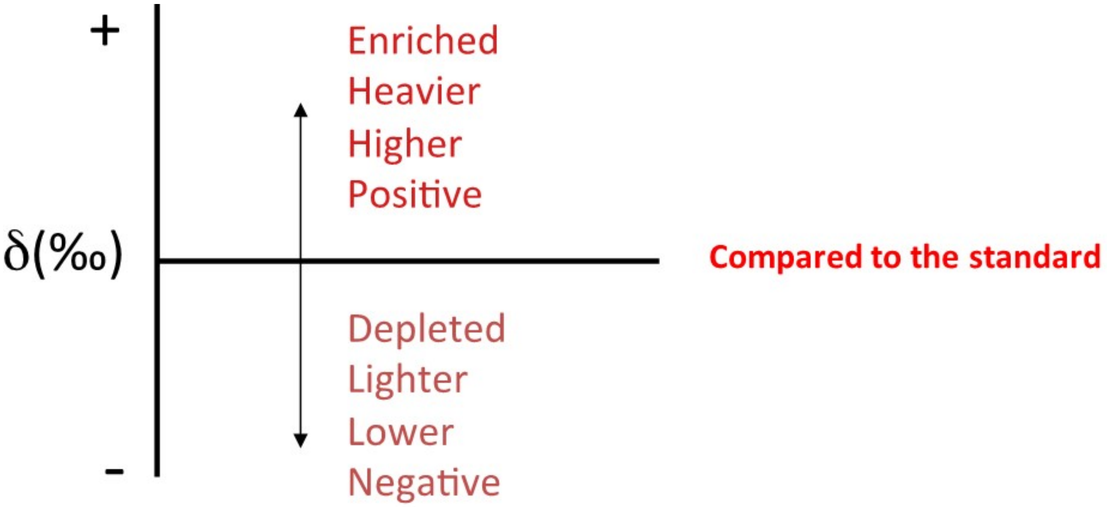

Figure 1-4: Terminology for describing stable isotope signatures.

The ^{13}C stable isotope measurement allows tracking the source of carbon in aquatic environments. For example, terrestrial plants fix atmospheric carbon dioxide during photosynthesis, which has a $\delta^{13}C$ signature of -7 to -8‰, while the source of carbon for marine plants (algae) is dissolved inorganic carbon (DIC) with a $\delta^{13}C$ signature of about 0‰. As both families of primary producers fix inorganic carbon through Rubisco, an enzyme that isotopically fractionate carbon by 20‰, this difference in source of carbon persists in the final isotopic signature of the bulk photosynthesized OM ($\delta^{13}C_{\text{terrestrial plants}}$ = -27‰ and $\delta^{13}C_{\text{marine}}$ = -20‰). The application of an Elemental Analyzer coupled to an isotope ratio mass spectrometer (EA-IRMS) for the purpose of measuring bulk elemental and isotopic signatures of OM is however relatively straightforward but interpretation of acquired data is sometimes very challenging.

1.8 Other proxies

Other proxies are regularly used in biogeochemistry to pinpoint the sources OM, or the history and reaction pathways that have affected a sample. The organic carbon to nitrogen molar ratio (C:N) is one of the primary tools used to indicate historical OM changes in sources of lake sediment. Terrestrial OM has a C:N greater than 20 while this ratio is between 4 and 10 for algae.[49] Increases in C:N ratios within sediment profiles normally reflect increases in the amount of terrestrial OM.[50,51] However, this proxy is not fully quantitative as the C:N of terrestrial OM decreases during early diagenesis (the physical and chemical changes occurring during the early stages of the conversion of sediment to sedimentary rock), whereas that of algae increases.[52] Regardless of its limitations, the atomic C:N ratio can provide useful insights into historical variations in the source of OM in sediment cores. In addition to ^{13}C, other stable isotopes (^{15}N, ^{18}O, ^{2}H) are commonly used in geochemistry. The combination of these proxies with bulk measurement approaches (FTIR, NMR and Scanning Transmission X-ray Microscopy (STXM)) allow acquisition of a better understanding of OM preservation.

1.9 Objectives of thesis

The main objectives of this work are to understand the role of the Fe-OC interactions in the preservation of OC in lake sediments, and to assess the importance of redox conditions in the formation of stable Fe-OC aggregates. We used sediments collected from Lake Tantaré, a freshwater aquatic system with two basins characterized by seasonally contrasting bottom water redox conditions. These differing redox conditions provide an opportunity to test our hypothesis regarding the importance of redox transitions in the formation of these stable OC-Fe complexes.

1.10 Arrangement of thesis

This thesis includes a general introduction (Chapter I), a soon-to-be submitted manuscript in Environmental Science and Technology (Chapter II), and a general conclusion (Chapter III). All chapters are formatted in the same manner with figures numbered consecutively.

Chapter I provides a general contextualization of the work carried out as part of the M.Sc. project. Chapter II ("Investigating organic matter preservation through complexation with iron oxides in Lake Tantaré") describes the comparison of the elemental (C, N, Fe), isotopic ($\delta^{13}C$, $\delta^{15}N$) and chemical (FTIR) composition of OM in two basins of Lake Tantaré to probe the importance of redox condition on the formation of iron-OM aggregates, as well as to assess whether high percentages of Fe-associated OC are found in this lake. A reductive extraction method was used to quantify the fraction of OM associated to iron in the sediments, and the composition of total OM, Fe-associated OM and residual OM is described. Finally, Chapter III provides concluding remarks in this project.

2 Investigating organic matter preservation through complexation with iron oxides in Lake Tantaré

Azadeh Joshani[1], Andrew Barber[1], Kathryn Balind[1], Charles Gobeil [2], and Yves Gélinas[1*]

[1] GEOTOP and Department of Chemistry and Biochemistry, Concordia University, 7141 Sherbrooke West, Montreal, QC, Canada, H4B 1R6

[2] INRS-Eau Terre Environment, 490 rue de la Couronne, Université du Québec, QC, Canada, G1K 9A9

* Corresponding author:
Yves Gélinas
Department of Chemistry and Biochemistry
Concordia University
7141 Sherbrooke Street West
Montréal, QC, Canada, H4B-1R6
Tel.: 514-848-2424, ext. 3337
Fax: 514-848-2868
Email: yves.gelinas@concordia.ca

List of keywords: Sediment, Iron, Organic carbon, Lake, Stable isotope, Oxic, Redox

2.1 Abstract

The biogeochemical cycles of iron (Fe) and organic carbon (OC) are closely interconnected. The concentration of reactive Fe is tightly controlled by soluble organic ligands in oceanic waters. In soil, Fe stabilizes OC by forming mixed aggregates that shield OC from degradation. In sediments however; the role of Fe in the preservation of OC is only starting to be explored. To quantify the amount of OC retained in the solid phase through its interaction with Fe, an approach based on the reductive dissolution of reactive solid phase Fe, was applied. In this work, we investigated Fe-OC interactions in lake sediments, using sediments collected from Lake Tantaré, an aquatic system with two basins characterized by contrasting bottom water redox conditions in the summer. These contrasting redox conditions provided an opportunity to assess the importance of oxic/anoxic interfaces in the formation of stable OC-Fe complexes. We found 30.1 ± 6.4% of OC directly associated with Fe minerals. We characterized the Fe-associated and the non-Fe-associated OC pools at the elemental (OC, total nitrogen), isotopic (δ^{13}C, δ^{15}N) and functional group (FTIR) levels. The differences between the two basins will be presented and discussed in relation to the working hypothesis. We found large differences in OC:Fe and TN:Fe ratios among the two basins which were not related to differences in OM chemical composition but rather to differences in reactive iron concentrations stemming from the higher abundance of mackinawite (FeS). Since the affinity of OM for mackinawite is much lower than for iron hydroxides, using OC:Fe and TN:Fe ratios as a diagnostic tool for the type of interactions between OM and Fe should be done with care in anoxic environment.

2.2 Introduction

Human activities have significantly affected the global carbon cycle over the past 200 years. The concentration of carbon dioxide (CO_2) in the atmosphere is now 30% higher than its level at the beginning of the Industrial Revolution, an increase that is responsible for the current global climate change.[53,54] The major pathway for atmospheric CO_2 removal is through photosynthesis of organic matter (OM) on land and in the surface ocean. In the ocean, most newly synthesized OM is rapidly oxidized back to inorganic carbon and eventually returns to the atmosphere as CO_2. As a result, only about 0.3% of the yearly oceanic primary production of organic carbon (OC) is ultimately buried and preserved in sediment.[7] Sedimentary burial and preservation of OC upholds the delicate balance of O_2 and CO_2 in the atmosphere on geological time scales[55] by maintaining the balance between primary production and respiration in the ocean as well as on land.[24] It also represents a long-term sink for redox-sensitive elements (such as C, N, S, Mn, and Fe) in global biogeochemical cycles.[13,48,56,57]

Several factors have been shown to play a role in long-term OC burial efficiency, such as OC degradation rate,[58] primary productivity,[13] sedimentation rate[59,60] and low bottom water oxygen concentration[22,61-63], but the exact controls on OM preservation still are not well-understood.[13] The close interactions between organic and inorganic sedimentary materials have long been recognized as one of the most important preservation mechanisms by which OC is physically protected through shielding, encapsulation or simple steric hindrance.[34,35] Physical protection is supported by the observation that more than 90% of preserved OC is very closely associated with minerals in most marine sediments[64] and can explain the long-term preservation of labile molecules such as peptides and carbohydrates in sediments.[36]

The interactions between organic and inorganic matter have traditionally been considered uniquely as chemical or physical adsorption processes on the surface of minerals such as clays. Such interactions are however reversible and cannot explain the long-term preservation of molecule that are labile when dissolved in sediment pore waters.[65] Lalonde et al. (2012) recently proposed a mechanism of physical protection through inner-sphere complexation reactions between organic compounds and nanophase iron oxide particles. These authors have estimated that an average of 21.5 ± 8.6% of the total OC in marine sediments, representing highly contrasting depositional settings, is directly attached to reactive solid iron phases.[48] Extrapolating to the global ocean, this estimate corresponds to a total mass of sedimentary OC directly associated to reactive iron of 19–45 $\times 10^{15}$ g.[48]

The concentrations of iron and OC co-vary in sediments[39] but elucidating the exact nature of the chemical bonds between OC and iron under contrasting redox conditions is extremely challenging because of the complicated chemistry of iron and OC near the sediment-water interface (SWI). In addition to chemi- and physisorption, sedimentary OM can interact with iron oxides through a ligand-exchange mechanism where electronegative functional groups such as carboxyl, phenol or alcohol exchange with the hydroxyl groups of iron oxide particles.[44,66] At the SWI, where oxygen from the water column diffuses through the uppermost layers of the sediment, the dominant Fe(III) phases include solid phase iron (hydr)oxides and other non-reducible iron containing clay minerals.[67] Below the oxic/anoxic interface where sediments are depleted in oxygen, iron(III) can be reductively dissolved to soluble iron(II) and diffuse either upwards towards the oxic zone where it is re-oxidized, or downward and precipitate as iron sulfide.[67] The re-oxidation of Fe(II) in the redox transition zone leads to the formation of iron hydroxide nanoparticles that interact strongly with OC owing to their chemical composition and high surface areas. While pH and competing anions (sulfate and phosphate in particular) dictate the adsorption of OM onto different types of iron oxides such as ferrihydrite, goethite and haematite,[44] complexation reactions between OM and iron nanoparticles would lead to the co-precipitation of surface-active Fe-OC aggregates. Aggregation of this type is analogous to the onion model of Mackey and Zirino (1994). It would result in a dramatic decrease in the reduction rate of Fe(III) under anoxic conditions, which would explain the persistence of reducible iron in anoxic sediments for thousands of years and to a decrease in OM degradation rates leading to higher OM burial efficiencies. [33,45]

Organic carbon burial and preservation in lentic ecosystems such as lakes, reservoirs, ponds and impoundments is poorly constrained because of the absence of comprehensive datasets, particularly for small water bodies. Recent studies have shown that the OC burial rates in these systems should be taken into account in global carbon cycle analyses even if they cover a small fraction of the Earth's land surface area.[9,10,68-70]

The main objectives of this work are to understand the role of the Fe-OC interactions in the preservation of OC in lake sediments, and to assess the importance of redox conditions in the formation of stable Fe-OC aggregates. We used sediments collected from Lake Tantaré, a freshwater aquatic system with two basins characterized by seasonally contrasting bottom water redox conditions. These differing redox conditions provide an opportunity to test our hypothesis regarding the importance of redox transitions in the formation of these stable OC-Fe complexes. The Fe-associated and the non-Fe-associated OC pools were characterized using elemental (organic carbon and total nitrogen) and isotopic ($\delta^{13}C$, $\delta^{15}N$) analysis, and their chemical composition was assessed by Fourier-transform infrared (FTIR) spectroscopy.

2.3 Materials and methods

2.3.1 Study site

Lake Tantaré (47°04′15″N, 71°33′42″ W) is a small (1.1 km^2) acidic (pH 5.4–7.0) and oligotrophic (Chl a 0.2–0.9 nM) lake located in an ecological reserve 40 km northwest of Québec City, in the province of Québec. This dimictic soft water lake, sitting on a granite and gneiss bedrock of the Canadian Precambrian Shield, is characterized by low concentrations of dissolved organic carbon (DOC; 2.2–2.8 mg L^{-1}).[37] Since the lake basin is uninhabited, metal ions are only introduced to this lake through natural weathering and long-range atmospheric deposition as the impact of wood harvesting or wildfire is negligible.[71] Lake Tantaré comprises four basins that are separated by shallow sills. In this study, we used sediments from Basin A, which is has maximum depth of 15 m and perennially oxic conditions (> 3.8 mg O_2 L^{-1}), as well as from Basin B, which has a maximum depth of 21 m and is characterized by seasonal variations in redox conditions as bottom waters become anoxic (< 0.01 mg O_2 L^{-1}) during late summer-early fall (Figure 2-1).[72-73]

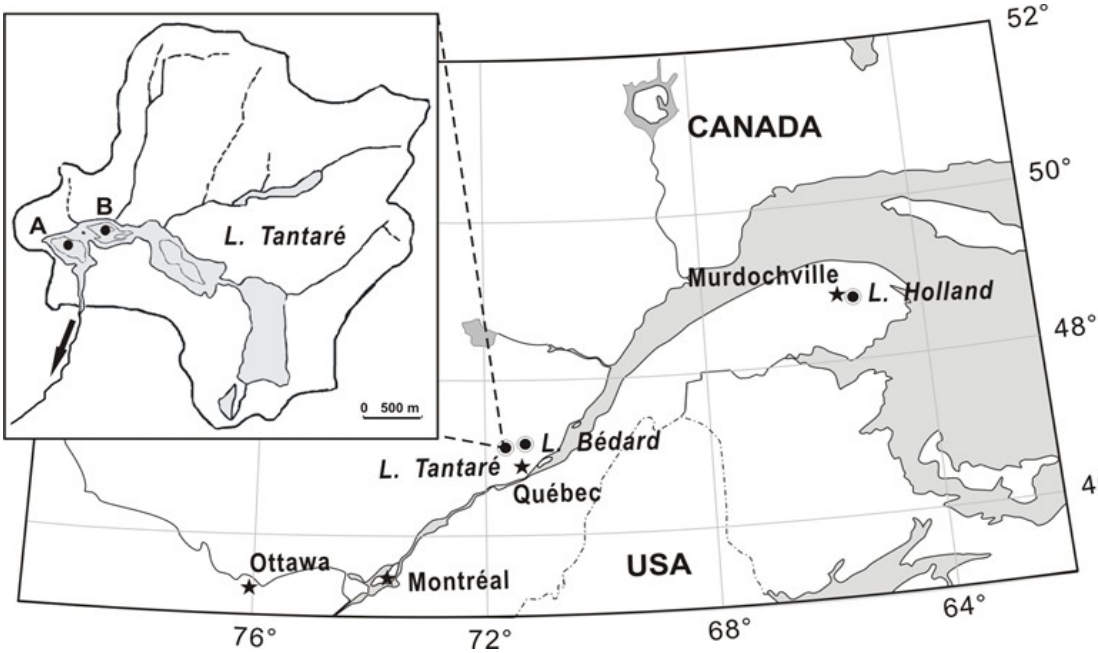

Figure 2-1: Map showing the location of Lakes Tantaré.[1]

2.3.2 Sampling

Sediment cores were collected in both basins in August 2013 using butyrate tubes with an inner diameter of 9.5 cm. Sediment were sliced at 0.5 or 1 cm intervals down to 15 (Basin A) or 25 cm (Basin B). The sediment samples were freeze-dried and then stored in polyethylene containers.

2.3.3 Extraction Method

The reductive extraction method used in this study was originally developed for quantifying reactive (reducible) iron in soils.[74] It was slightly modified to allow measurement of concomitant removal of OC (by elemental analysis coupled to an isotope ratio mass spectrometer, or EA-IRMS) and iron (by inductively coupled plasma mass spectrometry, or ICP-MS) from the marine and lake sediments.[48] In this method, dithionite is used to reductively solubilize Fe(III) oxides to Fe(II), along with citrate, a water-soluble complexing agent that keeps iron in solution, preventing re-adsorption to the solid phase. The reduction reaction was carried out under buffered conditions (bicarbonate) to maintain the pH at 7.3 (Appendix A). OC that was solubilized upon the reduction reaction was considered specifically associated with iron oxides as other reducible mineral phases such as manganese oxides were much less abundant in sediments. In order to take into account desorbed OC from sediment at the temperature and ionic strength used for the reduction reaction, a preliminary control experiment was performed on the sediment prior to the reduction step by replacing the citrate and dithionate with the mass of sodium chloride needed to obtain the same ionic strength as in reduction experiment (Appendix A).

2.3.4 EA-IRMS Measurements

OC and total nitrogen (TN) content as well as the stable $^{13}C/^{12}C$ and $^{15}N/^{14}N$ isotope ratios of the solid phase were measuredusing an elemental analyzer (EA, EuroVector 3028-HT) coupled to an Isoprime isotope ratio mass spectrometer (IRMS, GV Instruments, Manchester, England). The EA-IRMS calibration was done using an in-house pre-calibrated ß-alanine standard (%OC = 40.45%; %TN = 15.7%; $\delta^{13}C$ = -25.98 ± 0.23‰ and $\delta^{15}N$ = -2.21 ± 0.24‰) for both stable isotope measurements and concentration of carbon and nitrogen in bulk sediment.[43,75] The relative and absolute error for replicate measurements was better than 1% for OC and TN, and 0.3‰ for $\delta^{13}C$ and 0.5‰ for $\delta^{15}N$ signatures, respectively.[75] The %OC and $\delta^{13}C$ signatures were obtained before and after the removal of OM associated with iron oxide, and the signature of Fe-associated OC was calculated using a simple isotopic mass balance model. In order to remove inorganic carbon (i.e. carbonates) prior to EA-IRMS measurement, the freeze-dried sediment samples were weighed into silver capsules, exposed to 12 N HCl vapor for 12 hours, followed by a 1-hr heating step at 50°C and 6 hours in a desiccator to remove residual water/acid. The Ag capsules containing the decarbonated samples were then sealed and wrapped in a tin capsule before EA-IRMS analysis.

2.3.5 FTIR Measurements

FTIR analyses were carried out on the sediments before (initial) and after (residual) the removal of OM associated with iron oxide. Exactly 3 ± 0.1 mg of the freeze-dried sediment were homogenized with 100 ± 0.3 mg of potassium bromide using a mortar and pestle. All of homogenate was used to make a compressed pellet. Prior to acquiring the spectrum, the pellet chamber was purged nitrogen a minimum of 5 min to remove the carbon dioxide signal at 2350 cm^{-1}. The measurements were done on a Nicolet 6700 FTIR spectrophotometer (scan number: 128, resolution: 2 cm^{-1}). Furthermore, ICP-MS was used to measure iron concentration.

2.4 Results and discussion

2.4.1 Elemental and isotopic composition

The vertical distribution of OC, TN, reducible Fe concentrations, the C:N, OC:Fe molar ratios, the stable isotope signatures of carbon ($\delta^{13}C$) and nitrogen ($\delta^{15}N$) were determined in sediment cores of the perennially oxygenated basin (A) and a seasonally anoxic basin (B) of Lake Tantaré (Figure 2-2 and Figure 2-3). The total OC concentrations were similar in both basins and ranged between 22.4 ± 0.7 % and 27.1 ± 0.3 % for Basin A, and 21 ± 0.5 % to 26.8 ± 0.3 % for Basin B (Figure 2-2a), with small, generally synchronous variations in the past ~100 years which was consistent with the finding of Heiri et al. (2001) for the same lake. [76] These values are in agreement with the data reported by Feyte et al. (2010). The concentrations of OC associated with iron (Fe-associated OC) averaged 7.5 ± 1.6 % of the total sediment mass in the two basins (Figure 2-2a), corresponding on average to 30.1 ± 6.4 % of total organic carbon in Basins A and B. These values are similar to the results obtained for the only other lake sediments analyzed to date using this method, and are on the high end of the range of percentages measured for a series of marine sediments.[48] Noteworthy, despite of differences between the highest total OC concentration in Lalonde's sediment sample set (6.9 wt%) compared to Lake Tantaré sediment (20-28 wt%) the concentration of Fe-associated OC was similar in both sample set, which suggests that the conclusions reached for marine sediment also apply to organic-rich lake sediments.

Total nitrogen concentrations varied between 1.4 ± 0.45 % and 1.6 ± 0.39 % in Basin A, and 1.1 ± 0.48 % and 1.6 ± 0.39 % in Basin B (Figure 2-2b). TN concentrations were slightly lower at depth in Basin B compared to Basin A, but there was no difference when comparing the concentration of nitrogen associated to iron in two basins (Figure 2-2b). The concentrations of Fe-associated nitrogen varied between 0.15 and 0.50% in both basins, corresponding to between 20 and 30% of TN. This range is also consistent with the finding of Lalonde et al. for sediments of a boreal lake (21-34 %), but it is much higher than in marine sediments, for which the highest measured percentage of Fe-associated nitrogen was 15.28 ± 5.22 %, suggesting that the effect of iron on nitrogen dynamics is stronger in continental aquatic systems where OM is depleted in nitrogen.

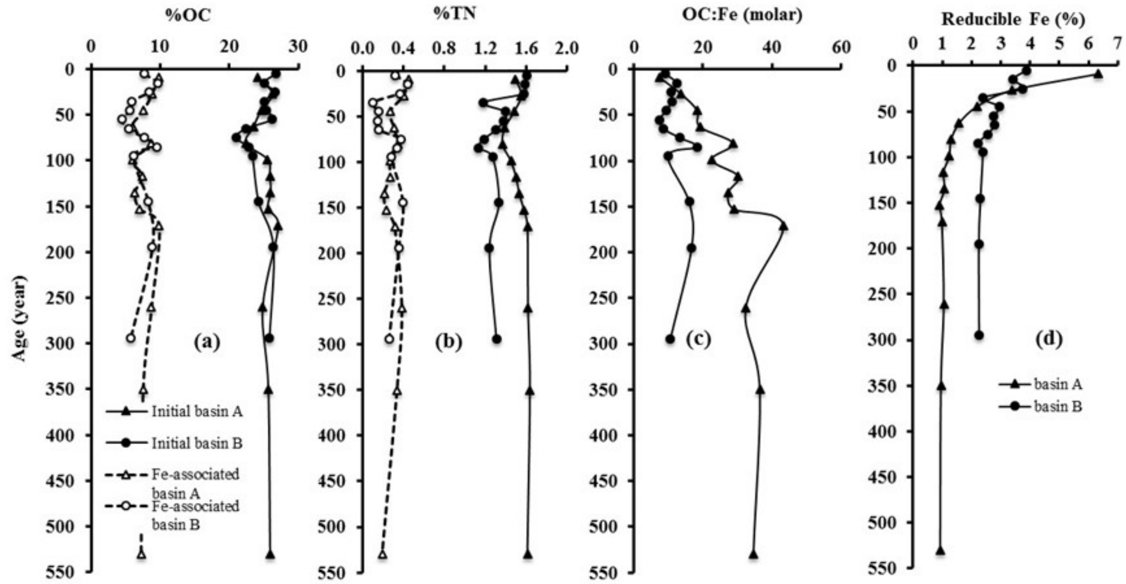

Figure 2-2: Age profiles of the percentage of the total sediment organic carbon (OC) bound to reactive iron phases (a) and %TN (b) before (Initial) and after extraction (Residual), OC:Fe molar ratio (c), and percent of reducible Fe in Basins A and B (d). Each point represents the average value of triplicate measurements.

High OC:Fe molar ratios were found in both basins, suggesting a tight linkage between biogeochemical cycles of OC and Fe in these samples. The ratios have remained similar in both basins for the past ~30 years, but they diverge considerably deeper in the sediment with averages of 26.4 ± 0.6 and 11.8 ± 0.7 for Basin A and B, respectively (Figure 2-2c). The differences in the OC:Fe and TN:Fe (data not shown) profiles between the two adjacent basins, each exposed to similar OC inputs but dissimilar oxygen exposure regimes, suggests two possible scenarios. First, the contrasting ratios could reflect differences in OC chemical composition driven by the different redox regimes in two basins, and second, they could be due to the presence of a pool of reactive iron with a much lower affinity for OM in Basin B, thus leading to lower OC:Fe ratios.

The average C:N molar ratios of total OM in Basins A and B are 19.3 ± 1.4 and 21.6 ± 1.1, respectively. These ratios are typical of soil OM and are higher than the ratios measured for setting particles of productive lake[77] (6-9), reflecting the predominance of allochthonous OM inputs in the sediments of Lake Tantaré.[78,79]

The higher C:N ratios for Fe-associated OM throughout the core in Basin A, and for sediment deposited in the past 85 years in Basin B, are driven by the depleted sediment nitrogen content, particularly in Basin B (Figure 2-3a and d). The higher ratios are due to the lower concentration of nitrogen in these samples, particularly in Basin B (Figure 2-2b). While several factors could explain the preferential removal of nitrogen-rich compounds over this interval, this observation agrees with the results from a long-term incubation experiment in which it was proposed that iron oxides lead to the preferential preservation of OC and, in parallel, to an enhancement in the removal of nitrogen-rich OM.[75]

The $\delta^{13}C$ and $\delta^{15}N$ stable isotope signatures for the total sediment OM as well as for the Fe-associated and residual OM fractions were similar and varied little with time in Basin A, aside from a 1 to 1.5 ‰ lower $\delta^{15}N$ signature for sediment deposited in the past ~100 years. This is not the case for Basin B where the $\delta^{13}C$ signature of Fe-associated OM was enriched by about 2 ‰ near the SWI, and depleted by as much as 3 ‰ in sediments deposited between 100-150 years ago (Figure 2-3e).

Two sharp peaks centered around 35 and 85 years characterized the $\delta^{15}N$ profile for total OM and the Fe-associated and residual fractions, with an enrichment as large as 3 ‰ at these depths where the TN concentration was also the lowest. This result agrees with the inverse relationship between TN and $\delta^{15}N$ in sediments from temperate lakes (Figure 2-3f).[80]

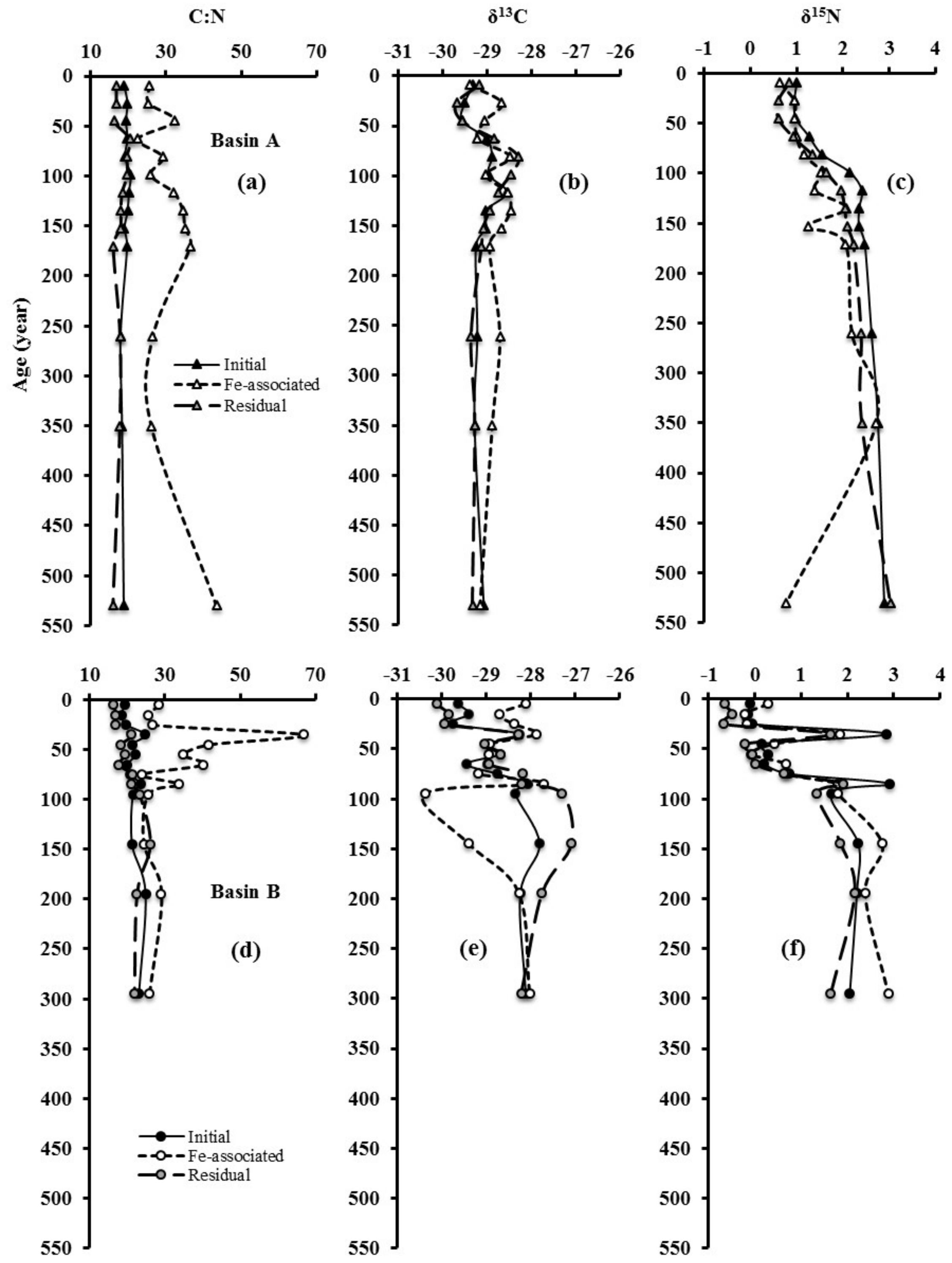

Figure 2-3: Age profiles of the atomic C:N ratio (a and d), carbon isotopic signatures ($\delta^{13}C$) (b and e) and nitrogen isotopic signatures $\delta^{15}N$ (c and f) of Initial and Residual sediments of Lake Tantaré Basins A and B, respectively.

2.4.2 OM chemical composition

The FTIR spectra of the total, residual and Fe-associated OM are presented, with an offset for better clarity, for the two basins in Figure 2-4. For each sample, the spectra for total OM and the control-treated samples were virtually indistinguishable from one another therefore the former were used for the discussion below. The OM lost during the control treatment was thus very similar in chemical composition to the non-extractable OM remaining after the treatment.

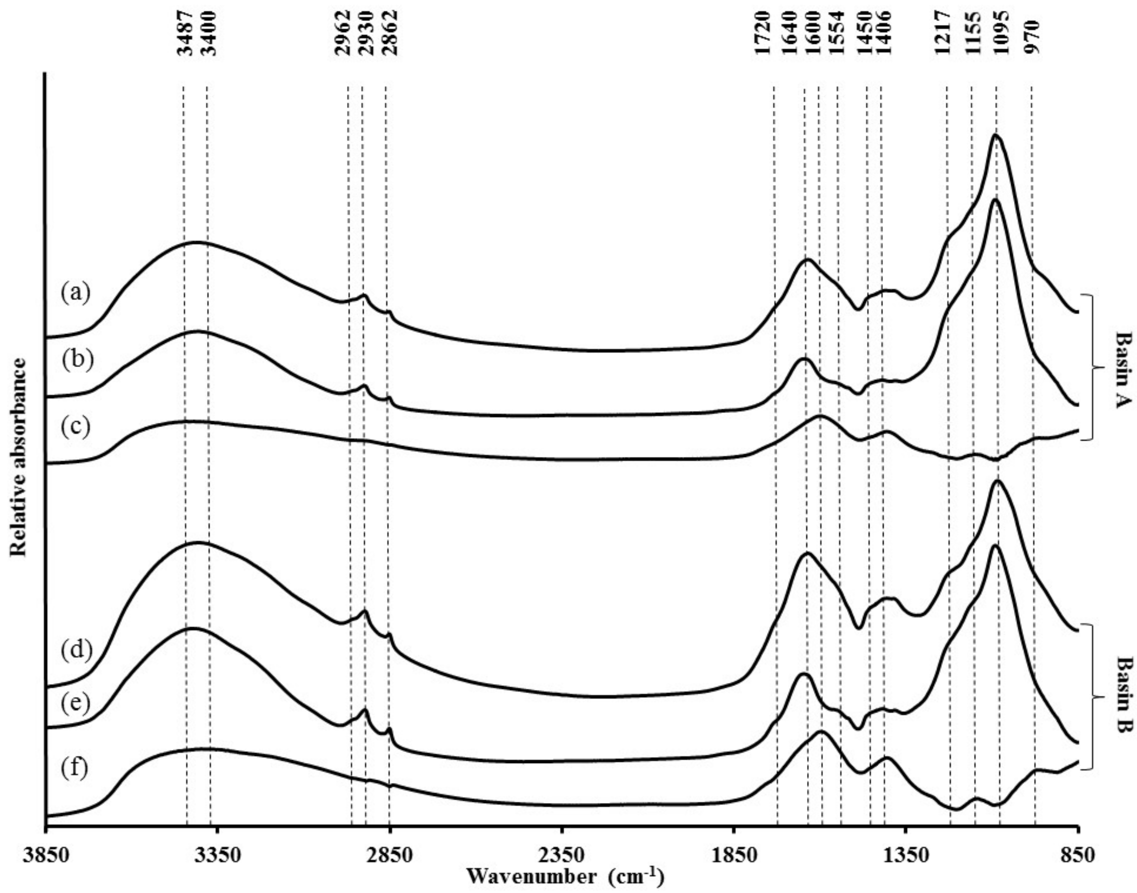

Figure 2-4: FTIR spectra of the Initial (a and d), Residual (b and e) and Fe-associated (c and f) OM for surface sediment (1-2 cm) of Basin A on top and Basin B at bottom.

The largest peak in the spectra at 1095 cm^{-1}, caused by the antisymmetric motion of silicon atoms (υ_{as}-Si-O-Si)[81] in Si-containing minerals (quartz and clays), was used as an internal standard to normalize the spectra since its abundance did not vary with depth in the sediments, and because Si-containing minerals are resistant to the dithionate treatment.[82] Combined with the precise and constant sediment-to-KBr mass ratio used when preparing the pellets, normalizing the spectra in this way allowed estimating the composition of the Fe-associated OM fraction by difference (spectrum before the reduction treatment minus spectrum after the treatment = spectrum of Fe-associated OM). The resulting three spectra were compared in order to assess differences such as wavelength shifts, variation in intensity or appearance of new peaks. No effort was made at deconvoluting and integrating (quantifying) the relative intensities of the different peaks owing to the uncertainty associated to the normalization, the spectra subtraction and the fact that several bands are not well resolved from their neighbour (shoulder). The comparison below therefore must be considered semi-quantitative.

A series of absorbance bands were present in all samples: (1) a broad band between 3800 and 2600 cm^{-1}, centered around 3450 cm^{-1}, corresponding to the stretching band of hydrogen in the O-H groups of alcohols, phenols, or carboxylic acids, as well as amide hydrogen stretching; (2) absorption bands representing C-H stretching of methyl and aldehyde functional groups near 2960, 2930 and 2860 cm^{-1}; (3) a shoulder at 1780 cm^{-1} for C=O stretch of COOH, asymmetric COO^- stretch at 1600 to 1650 cm^{-1}, symmetric COO^- stretch at 1400 to 1410 cm^{-1}(83); (4) bands corresponding to aromatic structures 1500 to 1620 cm^{-1} range; (5) the wavenumber region between 1470 and 1380 cm^{-1} is attributed to CH_2 and CH_3 bending; (6) a large band between 1000 and 1125 cm^{-1} corresponding to the stretching of C-O group for the tertiary, secondary, and primary alcohols at about 1150, 1120, and 1070 cm^{-1}.[84] Because of the presence of the intense silica band at 1095 cm^{-1}, the alcohol bands appear as shoulders on either side of the 1095 cm^{-1} band. No effort was made to exploit the bands below 1000 cm^{-1} because of the potential presence of bands attributable to minerals.

The infrared spectra of total OM were similar at each depth in the two basins (Figure 2-4, spectra a and d), with intensities relative to the silica band generally slightly lower at depth compared to the surface in both basins, as well as in Basin A compared to Basin B for equivalent depths (Figure B-1). The same was true for the Fe-associated (Figure B-2) and the residual (Figure B-3) OM. This result suggests that the contrasting bottom water redox conditions in the two basins did not lead to FTIR-visible differences in the speciation of sedimentary OM as the same functional groups with similar relative intensities were found in the different fractions of samples taken at equivalent depths. Also worth noting is the fact that the composition of the Fe-associated OM fraction, as well as that of the residual, non Fe-associated OM fractions remained similar over more than half a century as their composition remained constant with depth in each core (Figures B-2 and B-3). As the sediments are depleted in oxygen in both basins (except at the surface of Basin A), this result agrees with the reported long-term metastability of Fe-OM aggregates in anoxic settings, at least on century to millennium time scales (Lalonde et al. 2012).

There were however important differences when comparing the chemical composition of the three OM fractions for individual samples. While the differences in spectral peak shapes and intensities for total OM and residual OM were small, however the differences between these two fractions and Fe-associated OM, were clear. First, there was a clear change in peak shape and a shift of the O-H/N-H band between 3850 and 2600 cm^{-1} towards higher wavenumbers, with a maximum peak intensity shifted from 3450 to 3525 cm^{-1} for Basin A 19-20 cm

One of the most intriguing characteristic of Fe-associated OM is the almost complete absence on the C-H stretch (2960/2930/2860 cm^{-1}) and CH_2/CH_3 bending (1470/1380 cm^{-1}) bands (the latter two bands at 1470 and 1380 cm^{-1} appear as shoulders of the more intense 1410 cm^{-1} peak on the spectra of total and residual OM). These bands are present in most FTIR spectra of natural OM and point to highly aromatic or heteroatom organic structures associated with iron oxides.

The carbonyl and aromatic bands also differ in the Fe-associated OM spectra. First, a small shoulder at 1780 cm^{-1} is more clearly defined, although this could simply be due to the generally lower spectral relative abundances for Fe-associated OM. More importantly, there was a clear shift of the maximum intensity for the carboxyl asymmetric stretch peak from 1640 cm^{-1} in the spectrum for total OM to 1600 cm^{-1} in the spectrum for Fe-associated OM. Although aromatic C=C functional groups also have a stretching absorption in the same region (1600 cm^{-1}), the existence of a strong absorption band at 1400 cm^{-1}, which is more pronounced in the spectrum for Fe-associated OM, is consistent with the formation of metal-carboxylate complexes, as shown in several other studies.[44,83,85-88]

Interestingly, a small peak centered around 1150 cm^{-1} is apparent in the spectra of Fe-associated OM. This peak corresponds to tertiary alcohols as would be found in lignin phenols, which are known for their high affinity for iron oxides.[44,89,90] These spectral differences between Fe-associated OM and total or residual OM correspond to the functional groups lost when reductively removing the iron oxides. They provide clues to the type of compounds that readily associate with iron oxides in sediments and that remain part of the solid phase only because of their association with this mineral phase. These compounds are hydrophilic, aromatic- and carboxylic-rich, with tertiary O-H groups, analogous to lignin and tannin degradation products.

The FTIR analyses also provides information on the type of chemical bonds between the organic moieties and iron oxides[91] and demonstrates the importance of ligand exchange reactions as an important mechanism of complexation of sedimentary OM with Fe oxides, in agreement with the conclusions of Gu et al (1994). These results also suggest that complexation is taking place independently of sediment redox conditions, as long as a redox boundary exists where iron oxides can form in the presence of dissolved or particular OM (i.e. in the water column, as in basin B, or in the sediment/at the SWI as in Basin A). Complexation and adsorption of OM on the surface of iron oxides are thus complementary mechanisms of association between Fe oxides and OM, whose relative importance depends on local conditions (mostly oxide-reduction potential, but also the abundance of iron, OM and competing ligands such as sulfides). More work is needed to fully understand the fine controls on these competing reactions in sedimentary environments. Noteworthy, the similar chemical composition of Fe-associated OM in both basins and at different depths suggests that the large differences in OC:Fe and TN:Fe ratios measured between the two basins were not linked to differences in OM abundance, composition or reactivity, but rather to differences linked to Fe cycling in the two basins.

2.4.3 Iron

Reducible Fe concentrations were high below the SWI in Basin A (276.8 ± 6.1 µM, or 6.3% of the total mass) and decreased sharply to 86.8 ± 1.9 µM at 2-3 cm of depth (corresponding to an age of 45 yrs.) to reach nearly constant concentrations deeper in the sediment (Figure 2-2d). The enrichment of Fe(III) oxyhydroxides (poorly crystalline ferrihydrite, lepidocrocite and goethite) below the SWI agrees with previous studies conducted in the same basin[1,73,92-94] and is due to the recycling of Fe at depth (partial dissolution of Fe(III) oxides, release of dissolved Fe(II) to pore waters, followed by its migration towards the near surface oxic layer where it is re-oxidized to Fe(III) oxides, and at depth where it can react with dissolved sulphides to form mackinawite or pyrite).[37,95] As also observed by Feyte et al. (2010), dissolved Fe(II) in the pore waters of Basin B likely is lost through diffusion to the water column owing to the absence of an oxic sediment layer near the SWI, hence explaining the absence of an enrichment in Fe(III) oxyhydroxides in this core. The downward diffusing Fe(II) reacting with sulphide may however explain the higher reactive iron concentrations in this core given the more reducing conditions in sediments of Basin B compared to Basin A, and the absence of a Fe(III) oxyhydroxides sink near the SWI. Indeed, while Couture et al. (2010) reported that the concentration of acid volatile sulfides (AVS) were low and thus contributed little to reduced Fe solid phases in Basin A, AVS concentrations were about an order of magnitude higher in Basin B (Gobeil, unpublished data). Mackinawite, a form of AVS resulting from the reaction of dissolved Fe(II) and sulphides in the pore water, is highly unstable under oxic conditions. Their oxidation to iron oxides during sample preparation and storage likely contributed to the reactive iron pool in Basin B, artificially decreasing the measured OC:Fe since the formation of mackinawite from Fe(II) and HS^- under anoxic conditions, and in the presence of terrestrial dissolved OC, leads to the formation of precipitates with a maximum OC:Fe ratio of about 1 (unpublished data).

There are several implications to our results. First, the mechanism reported by Lalonde et al. (2012) for marine sediments also plays an important role in lacustrine sediments, as shown in Lake Tantaré where about 30% of the total OC is closely associated with iron oxides. Second, redox conditions are not the main factor explaining the formation of Fe-OM aggregates, but a redox boundary where Fe(II) is oxidized to Fe(III) and precipitated as amorphous iron oxide phases in the presence of dissolved OC most likely is key. These aggregates appear stable on very long time-scales under anoxic conditions, likely because the Fe oxides are poisoned by co-precipitated OC, making them less readily available to iron-reducing bacteria and reductive dissolution. They are, however, probably degraded when exposed to oxidizing conditions on long time scales through non-specific OM oxidation reactions involving activated oxygen species. This Fe-OM complexation mechanism thus acts as a shuttle that actively transfers reactive OC from oxic to anoxic settings while partially protecting it from enzymatic chemolytic attack.[75] Third, the formation of Fe-OM aggregates is not driven by OM composition as there were no compositional differences in Fe-associated OM between cores of sediment depths. Fourth, iron sulfides may contribute to the measured reactive Fe pool and may therefore artificially lower the OC:Fe ratios measured using this method. Thus care must be taken when using OC:Fe ratios as a diagnostic tool in reducing sediments to apportion complexation (inner-sphere) and adsorption (outer-sphere) reactions, as done by Lalonde et al. (2012). OC:Fe ratios should be used only in sediments accumulated under oxic conditions.

More work is needed to untangle the complex web of reactions involving OM and Fe in sediments, including the kinetics of the competing reactions and the interaction between organic matter and iron-sulphite minerals, especially mackinawite (FeS). Importantly, studies such as this one focusing on the chemistry of Fe-OM interactions should be paralleled by others assessing the role of bacteria in the direct and indirect formation and degradation of Fe-OM complexes.

3 General conclusion

Our study is the first to look at differences in the interactions between OM and iron oxides in sediment cores from two adjacent basins in Lake Tantaré, each exposed to similar OM inputs, but characterized by contrasting oxidation-reduction regimes. In marine environments, these interactions accounted for the preservation of approximately 4000 times more C than the atmospheric pool.[48] Historically, global carbon budgets neglected to include inland water systems as a significant sink for OC on the planet, yet the complex redox transitions found within marine sedimentary environments allowing for the sequestration of OM through interactions with redox sensitive metal oxides, also occur within lake sediments. Recent approximations show that despite the low surface coverage of lentic systems, the high OC burial rates make them a significant contributor to the global carbon cycle.[68] As such, the main thrust of our research was to understand the effect of redox conditions on the elemental, isotopic and chemical composition of Fe-associated OM in Lake Tantaré.

We found that 30.1 ± 6.4 % of OC is associated with iron oxides in lake sediments, comparatively higher than what has been reported for marine sediments (21.5 ± 8.6 %).[48] Even though some global scale studies have reviewed specific processes such as the exchange of carbon dioxide with the atmosphere and carbon burial, most studies of lake carbon cycling are from single systems. Focusing only on a specific environment and not accounting for all of the main terms in OC inputs and outputs results in an incomplete and uncertain OC budget for most lakes.[96] Our research suggests that lakes have a critical effect on OC preservation, however the fundamental budgetary data needed to estimate the global budget of preserved OC in lakes is incomplete.

Our work also showed that bottom water redox conditions play a small role in determining the chemical composition of OM associated with iron oxides both in terms of chemical or isotopical composition. The similarity between chemical compositions of OM associated with Fe in two contrasting redox basins, as well as at different depths in sediment cores suggests that the nature of the interactions between Fe and OM is non-specific at least in Lake Tantaré. Moreover, the FTIR data indicates that, in terms of the nature of the bonds, inner-sphere interaction between Fe and OM or co-precipitation also play a role in lakes.

Up until now, interaction mechanisms between the iron oxides and OM have been inferred from the OC:Fe molar ratio of the DCB (Dithionite-Citrate-Bicarbonate) post extraction supernatant. Our results clearly indicate that using OC:Fe molar ratios is not appropriate in reducing settings as the reactive iron concentration will be affected by factors not linked to Fe-OM interactions, such as the buildup of FeS_x under anoxic conditions. A better understanding of the preservative effects of iron sulfide species on OM would be required in order to re-evaluate the calculated OC:Fe ratios.

Future directions

In light of the results, more work is needed to verify whether the high value of Fe-associated OC observed in Lake Tantaré and Lake Brock are truly representative of most inland fresh water bodies. Up until now, the preservative interactions between OC and Fe have only been studied in these two lakes, therefore additional sampling in other contrasting lakes, that have similar OM input but different oxygen exposure regime should be initiated.

Future research strategies should be specifically directed at delineating the mechanisms for interaction between OM and Fe-S minerals. In particular, special effort is needed to determine the quality and quantity of sorbed OM to the surface of Fe-S minerals such as mackinawite. One of the questions that should be answered is that whether iron sulfide phases have the same protecting effect as iron oxide species and how much OC is associated to these species. We are currently investigating this possibility through the precipitation of iron sulfur species in the presence of OM while varying molar ratios of Fe-S to OM and pH.

Bulk organic extraction and spectroscopic analysis were used in this work to determine the chemical composition of sediment OM. However the majority of sediment OM is categorized as molecularly uncharacterizable (MUC-OM)[24], which cannot be quantified or identified with these techniques. The extraction procedure outlined in this text coupled with the FT-IR analysis allowed us to characterize the bulk chemical composition of the OM associated to reactive iron species. Techniques looking at intact sediment material without any previous harsh sample preparation could be used in order to better characterize OM in relation to its preservation within the mineral matrix.

Application of novel techniques such as Scanning Transmission X-ray Microscopy (STXM) can reduce the artefacts associated with other methods during sample preparation. Although, there are many limitations of this technique for low OC, high mineral content samples, STXM is the ideal tool for examining the physico-chemical interplay between OM and the sediment mineral matrix on unadulterated sediment particles making the analysis of complex OM samples possible at the nm scale.

Finally, the physical/chemical characteristics of these Fe-OM complexes must be assessed under reducing conditions from both a thermodynamic stability and kinetics of formation/dissolution perspective. This would lead to a better understanding of the mechanism of formation, nature of the interactions and favourable formation/dissolution conditions for these complexes. Although decades of research have gone into the interplay between the biogeochemical cycles of iron and carbon in marine sediments, the importance of iron as a key regulator of the lacustrine sediment OM pool has only begun to be investigated.

References

1 Feyte, S., Gobeil, C., Tessier, A. & Cossa, D. Mercury dynamics in lake sediments. *Geochimica et Cosmochimica Acta* **82**, 92-112 (2012).

2 Collins, M., Knutti, R., Arblaster, J., Dufresne, J.-L., Fichefet, T., Friedlingstein, P., Gao, X., Gutowski, W., Johns, T. & Krinner, G. Long-term climate change: projections, commitments and irreversibility. (Cambridge University Press, 2013).

3 Kump, L. R., Bralower, T. J. & Ridgwell, A. Ocean acidification in deep time. *Oceanography* **22**, 94-107 (2009).

4 Lüthi, D., Le Floch, M., Bereiter, B., Blunier, T., Barnola, J.-M., Siegenthaler, U., Raynaud, D., Jouzel, J., Fischer, H. & Kawamura, K. High-resolution carbon dioxide concentration record 650,000–800,000 years before present. *Nature* **453**, 379-382 (2008).

5 Pagani, M., Zachos, J. C., Freeman, K. H., Tipple, B. & Bohaty, S. Marked decline in atmospheric carbon dioxide concentrations during the Paleogene. *Science* **309**, 600-603 (2005).

6 Solomon, S. Climate change 2007-the physical science basis: Working group I contribution to the fourth assessment report of the IPCC. Vol. 4 (Cambridge University Press, 2007).

7 Galy, V., France-Lanord, C., Beyssac, O., Faure, P., Kudrass, H. & Palhol, F. Efficient organic carbon burial in the Bengal fan sustained by the Himalayan erosional system. *Nature* **450**, 407-410 (2007).

8 Cole, J. J. & Caraco, N. F. Emissions of nitrous oxide (N2O) from a tidal, freshwater river, the Hudson River, New York. *Environmental Science & Technology* **35**, 991-996 (2001).

9 Sobek, S., Algesten, G., Bergstrom, A. K., Jansson, M. & Tranvik, L. J. The catchment and climate regulation of pCO2 in boreal lakes. *Global Change Biology* **9**, 630-641 (2003).

10 Pace, M. L. & Prairie, Y. T. Respiration in lakes. *Respiration in aquatic ecosystems*, 103-121 (Oxford University Press, 2005).

11 Wang, M., Chen, H., Yu, Z., Wu, J., Zhu, Q. a., Peng, C., Wang, Y. & Qin, B. Carbon accumulation and sequestration of lakes in China during the Holocene. *Global Change Biology*, doi:10.1111/gcb.13055 (2015).

12 Berner, R. A. Early diagenesis: A theoretical approach. (Princeton University Press, 1980).

13 Hedges, J. I. & Keil, R. G. Sedimentary organic matter preservation: an assessment and speculative synthesis. *Marine Chemistry* **49**, 81-115 (1995).

14 Henrichs, S. M. Early diagenesis of organic matter in marine sediments: progress and perplexity. *Marine Chemistry* **39**, 119-149 (1992).

15 Hart, P. J. The Earth's crust and upper mantle: structure, dynamic processes, and their relation to deep-seated geological phenomena. (American Geophysical Union, 1969).

16 Silva, A. J., Hollister, C. D., Laine, E. P. & Beverly, B. E. Geotechnical properties of deep sea sediments: Bermuda Rise. *Marine Georesources & Geotechnology* **1**, 195-232 (1976).

17 Wakeham, S. G. & Lee, C. in *Organic geochemistry* 145-169 (Springer, 1993).

18 Wüst, R. A., Ward, C. R., Bustin, R. M. & Hawke, M. I. Characterization and quantification of inorganic constituents of tropical peats and organic-rich deposits from Tasek Bera (Peninsular Malaysia): implications for coals. *International journal of coal geology* **49**, 215-249 (2002).

19 Ransom, B., Kim, D., Kastner, M. & Wainwright, S. Organic matter preservation on continental slopes: importance of mineralogy and surface area. *Geochimica et Cosmochimica Acta* **62**, 1329-1345 (1998).

20 Burdige, D. J. & Gardner, K. G. Molecular weight distribution of dissolved organic carbon in marine sediment pore waters. *Marine Chemistry* **62**, 45-64 (1998).

21 Pedersen, T. & Calvert, S. Anoxia vs. productivity: what controls the formation of organic-carbon-rich sediments and sedimentary Rocks? *AAPG Bulletin* **74**, 454-466 (1990).

22 Demaison, G. & Moore, G. T. Anoxic environments and oil source bed genesis. *AApG Bulletin* **64**, 1179-1209 (1980).

23 Gélinas, Y., Baldock, J. A. & Hedges, J. I. Organic carbon composition of marine sediments: effect of oxygen exposure on oil generation potential. *Science* **294**, 145-148 (2001).

24 Burdige, D. J. Preservation of organic matter in marine sediments: controls, mechanisms, and an imbalance in sediment organic carbon budgets? *Chemical reviews* **107**, 467-485 (2007).

25 Aller, R. C. & Mackin, J. E. Preservation of reactive organic matter in marine sediments. *Earth and planetary science letters* **70**, 260-266 (1984).

26 Rimmer, S. M., Thompson, J. A., Goodnight, S. A. & Robl, T. L. Multiple controls on the preservation of organic matter in Devonian–Mississippian marine black shales: geochemical and petrographic evidence. *Palaeogeography, Palaeoclimatology, Palaeoecology* **215**, 125-154 (2004).

27 Cowie, G. The biogeochemistry of Arabian Sea surficial sediments: A review of recent studies. *Progress in Oceanography* **65**, 260-289 (2005).

28 Zonneveld, K., Versteegh, G., Kasten, S., Eglinton, T. I., Emeis, K.-C., Huguet, C., Koch, B., de Lange, G. J., De Leeuw, J. & Middelburg, J. J. Selective preservation of organic matter in marine environments; processes and impact on the sedimentary record. *Biogeosciences* **7**, 483-511 (2010).

29 Tissot, B., Durand, B., Espitalie, J. & Combaz, A. Influence of nature and diagenesis of organic matter in formation of petroleum. *AAPG Bulletin* **58**, 499-506 (1974).

30 Thurman, E. M. Organic Geochemistry of Natural Waters (Springer Netherlands, 1985).

31 Tegelaar, E., De Leeuw, J., Derenne, S. & Largeau, C. A reappraisal of kerogen formation. *Geochimica et Cosmochimica Acta* **53**, 3103-3106 (1989).

32 Knicker, H. Stabilization of N-compounds in soil and organic-matter-rich sediments what is the difference? *Marine Chemistry* **92**, 167-195 (2004).

33 Jones, D. & Edwards, A. Influence of sorption on the biological utilization of two simple carbon substrates. *Soil Biology and Biochemistry* **30**, 1895-1902 (1998).

34 Arnarson, T. S. & Keil, R. G. Changes in organic matter–mineral interactions for marine sediments with varying oxygen exposure times. *Geochimica et Cosmochimica Acta* **71**, 3545-3556 (2007).

35 Ingalls, A. E., Lee, C., Wakeham, S. G. & Hedges, J. I. The role of biominerals in the sinking flux and preservation of amino acids in the Southern Ocean along 170 W. *Deep Sea Research Part II: Topical Studies in Oceanography* **50**, 713-738 (2003).

36 Kennedy, M. J. & Wagner, T. Clay mineral continental amplifier for marine carbon sequestration in a greenhouse ocean. *Proceedings of the National Academy of Sciences* **108**, 9776-9781 (2011).

37 Liu, K., Wu, L., Couture, R.-M., Li, W. & Van Cappellen, P. Iron isotope fractionation in sediments of an oligotrophic freshwater lake. *Earth and Planetary Science Letters* **423**, 164-172 (2015).

38 Rue, E. L. & Bruland, K. W. Complexation of iron (III) by natural organic ligands in the Central North Pacific as determined by a new competitive ligand equilibration/adsorptive cathodic stripping voltammetric method. *Marine Chemistry* **50**, 117-138 (1995).

39 Berner, R. A. Sedimentary pyrite formation. *American Journal of Science* **268**, 1-23 (1970).

40 Kaiser, K. & Guggenberger, G. The role of DOM sorption to mineral surfaces in the preservation of organic matter in soils. *Organic Geochemistry* **31**, 711-725 (2000).

41 Deflandre, B., Mucci, A., Gagné, J.-P., Guignard, C. & jørn Sundby, B. Early diagenetic processes in coastal marine sediments disturbed by a catastrophic sedimentation event. *Geochimica et Cosmochimica Acta* **66**, 2547-2558 (2002).

42 Johnson, K. S., Gordon, R. M. & Coale, K. H. What controls dissolved iron concentrations in the world ocean? *Marine Chemistry* **57**, 137-161 (1997).

43 Ouellet, A., Lalonde, K., Plouhinec, J. B., Soumis, N., Lucotte, M. & Gélinas, Y. Assessing carbon dynamics in natural and perturbed boreal aquatic systems. *Journal of Geophysical Research* **117,** G001943-G001956 (2012).

44 Gu, B., Schmitt, J., Chen, Z., Liang, L. & McCarthy, J. F. Adsorption and desorption of natural organic matter on iron oxide: mechanisms and models. *Environmental Science & Technology* **28**, 38-46 (1994).

45 Boudot, J., Hadj, A. B., Steiman, R. & Seigle-Murandi, F. Biodegradation of synthetic organo-metallic complexes of iron and aluminium with selected metal to carbon ratios. *Soil Biology and Biochemistry* **21**, 961-966 (1989).

46 van der Zee, C., Roberts, D. R., Rancourt, D. G. & Slomp, C. P. Nanogoethite is the dominant reactive oxyhydroxide phase in lake and marine sediments. *Geology* **31**, 993-996 (2003).

47 Katsev, S., Chaillou, G., Sundby, B. & Mucci, A. Effects of progressive oxygen depletion on sediment diagenesis and fluxes: A model for the lower St. Lawrence River Estuary. *Limnology and Oceanography* **52**, 2555-2568 (2007).

48 Lalonde, K., Mucci, A., Ouellet, A. & Gélinas, Y. Preservation of organic matter in sediments promoted by iron. *Nature* **483**, 198-200 (2012).

49 Mayer, L. M. Surface area control of organic carbon accumulation in continental shelf sediments. *Geochimica et Cosmochimica Acta* **58**, 1271-1284 (1994).

50 Guilizzoni, P., Marchetto, A., Lami, A., Cameron, N., Appleby, P., Rose, N., Schnell, Ø., Belis, C., Giorgis, A. & Guzzi, L. The environmental history of a mountain lake (Lago Paione Superiore, Central Alps, Italy) for the last c. 100 years: a multidisciplinary, palaeolimnological study. *Journal of Paleolimnology* **15**, 245-264 (1996).

51 Kansanen, P. H. & Jaakkola, T. in *Annales Zoologici Fennici* **22**, 13-55 (1985).

52 Meyers, P. A., Leenheer, M. J., Eaoie, B. & Maule, S. Organic geochemistry of suspended and settling particulate matter in Lake Michigan. *Geochimica et Cosmochimica Acta* **48**, 443-452 (1984).

53 Falkowski, P., Scholes, R., Boyle, E. e. a., Canadell, J., Canfield, D., Elser, J., Gruber, N., Hibbard, K., Högberg, P. & Linder, S. The global carbon cycle: a test of our knowledge of earth as a system. *Science* **290**, 291-296 (2000).

54 Vitousek, P. M., Mooney, H. A., Lubchenco, J. & Melillo, J. M. Human domination of Earth's ecosystems. *Science* **277**, 494-499 (1997).

55 Hartnett, H. E., Keil, R. G., Hedges, J. I. & Devol, A. H. Influence of oxygen exposure time on organic carbon preservation in continental margin sediments. *Nature* **391**, 572-575 (1998).

56 Thamdrup, B., Fossing, H. & Jørgensen, B. B. Manganese, iron and sulfur cycling in a coastal marine sediment, Aarhus Bay, Denmark. *Geochimica et Cosmochimica Acta* **58**, 5115-5129 (1994).

57 Straub, K. L., Benz, M., Schink, B. & Widdel, F. Anaerobic, nitrate-dependent microbial oxidation of ferrous iron. *Applied and Environmental Microbiology* **62**, 1458-1460 (1996).

58 Canfield, D. E. Factors influencing organic carbon preservation in marine sediments. *Chemical Geology* **114**, 315-329 (1994).

59 Müller, P. J. & Suess, E. Productivity, sedimentation rate, and sedimentary organic matter in the oceans I. Organic carbon preservation. *Deep Sea Research Part A. Oceanographic Research Papers* **26**, 1347-1362 (1979).

60 Henrichs, S. M. & Reeburgh, W. S. Anaerobic mineralization of marine sediment organic matter: rates and the role of anaerobic processes in the oceanic carbon economy. *Geomicrobiology Journal* **5**, 191-237 (1987).

61 Betts, J. & Holland, H. The oxygen content of ocean bottom waters, the burial efficiency of organic carbon, and the regulation of atmospheric oxygen. *Palaeogeography, Palaeoclimatology, Palaeoecology* **97**, 5-18 (1991).

62 Paropkari, A. L., Babu, C. P. & Mascarenhas, A. A critical evaluation of depositional parameters controlling the variability of organic carbon in Arabian Sea sediments. *Marine Geology* **107**, 213-226 (1992).

63 Hartnett, H. E. & Devol, A. H. Role of a strong oxygen-deficient zone in the preservation and degradation of organic matter: A carbon budget for the continental margins of northwest Mexico and Washington State. *Geochimica et Cosmochimica Acta* **67**, 247-264 (2003).

64 Kell, R. G., Montluçon, D. B. & Prahli, F. G. organic matter in marine sediments. *Nature* **370**, 18 (1994).

65 Mayer, L. M. Sedimentary organic matter preservation: an assessment and speculative synthesis a comment. *Marine Chemistry* **49**, 123-126 (1995).

66 Kaiser, K., Guggenberger, G., Haumaier, L. & Zech, W. Dissolved organic matter sorption on sub soils and minerals studied by 13C-NMR and DRIFT spectroscopy. *European Journal of Soil Science* **48**, 301-310 (1997).

67 Viollier, E., Inglett, P., Hunter, K., Roychoudhury, A. & Van Cappellen, P. The ferrozine method revisited: Fe (II)/Fe (III) determination in natural waters. *Applied Geochemistry* **15**, 785-790 (2000).

68 Clow, D. W., Stackpoole, S. M., Verdin, K. L., Butman, D. E., Zhu, Z., Krabbenhoft, D. P. & Striegl, R. G. Organic Carbon Burial in Lakes and Reservoirs of the Conterminous United States. *Environmental Science & Technology* (2015).

69 Ferland, M. E., Giorgio, P. A., Teodoru, C. R. & Prairie, Y. T. Long-term C accumulation and total C stocks in boreal lakes in northern Québec. *Global Biogeochemical Cycles* **26** (2012).

70 Cole, J. J., Cole, J. J., Caraco, N. F. & Caraco, N. F. Carbon in catchments: connecting terrestrial carbon losses with aquatic metabolism. *Marine and Freshwater Research* **52**, 101-110 (2001).

71 Alfaro-De la Torre, M. C., Beaulieu, P.-Y. & Tessier, A. In situ measurement of trace metals in lakewater using the dialysis and DGT techniques. *Analytica Chimica Acta* **418**, 53-68 (2000).

72 Couture, R.-M., Gobeil, C. & Tessier, A. Chronology of atmospheric deposition of arsenic inferred from reconstructed sedimentary records. *Environmental Science & Technology* **42**, 6508-6513 (2008).

73 Couture, R.-M., Shafei, B., Van Cappellen, P., Tessier, A. & Gobeil, C. Non-steady state modeling of arsenic diagenesis in lake sediments. *Environmental Science & Technology* **44**, 197-203 (2009).

74 Mehra, O. & Jackson, M. *National Conference on Clays and Clays Minerals.* 317-327.

75 Barber, A., Lalonde, K., Mucci, A. & Gélinas, Y. The role of iron in the diagenesis of organic carbon and nitrogen in sediments: A long-term incubation experiment. *Marine Chemistry* **162**, 1-9 (2014).

76 Heiri, O., Lotter, A. F. & Lemcke, G. Loss on ignition as a method for estimating organic and carbonate content in sediments: reproducibility and comparability of results. *Journal of Paleolimnology* **25**, 101-110 (2001).

77 Hamilton-Taylor, J., Willis, M. & Reynolds, C. Depositional fluxes of metals and phytoplankton in Windermere as measured by sediment traps1. *Limnology and Oceanography* **29**, 695-710 (1984).

78 Bordovskiy, O. Transformation of organic matter in bottom sediments and its early diagenesis. *Marine Geology* **3**, 83-114 (1965).

79 Thornton, S. & McManus, J. Application of organic carbon and nitrogen stable isotope and C/N ratios as source indicators of organic matter provenance in estuarine systems: evidence from the Tay Estuary, Scotland. *Estuarine, Coastal and Shelf Science* **38**, 219-233 (1994).

80 Botrel, M., Gregory-Eaves, I. & Maranger, R. Defining drivers of nitrogen stable isotopes ($\delta^{15}N$) of surface sediments in temperate lakes. *Journal of Paleolimnology* **52**, 419-433 (2014).

81 Swann, G. E. & Patwardhan, S. Application of Fourier Transform Infrared Spectroscopy (FTIR) for assessing biogenic silica sample purity in geochemical analyses and palaeoenvironmental research. *Climate of the Past* **7**, 65-74 (2011).

82 Kovač, N., Faganeli, J., Bajt, O., Šket, B., Vuk, Š., Orel, B. & Mozetič, P. Degradation and preservation of organic matter in marine macroaggregates. *Acta. Chimica Slovenica* **53**, 81-87 (2006).

83 Chorover, J. & Amistadi, M. K. Reaction of forest floor organic matter at goethite, birnessite and smectite surfaces. *Geochimica et Cosmochimica Acta* **65**, 95-109 (2001).

84 Stevenson, F. J. Humus chemistry: genesis, composition, reactions. (John Wiley & Sons, 1994).

85 Biber, M. V. & Stumm, W. An in-situ ATR-FTIR study: The surface coordination of salicylic acid on aluminum and iron (III) oxides. *Environmental Science & Technology* **28**, 763-768 (1994).

86 Eusterhues, K., Rennert, T., Knicker, H., Kögel-Knabner, I., Totsche, K. U. & Schwertmann, U. Fractionation of organic matter due to reaction with ferrihydrite:

coprecipitation versus adsorption. *Environmental Science & Technology* **45**, 527-533 (2010).

87 Guan, X.-H., Shang, C. & Chen, G.-H. ATR-FTIR investigation of the role of phenolic groups in the interaction of some NOM model compounds with aluminum hydroxide. *Chemosphere* **65**, 2074-2081 (2006).

88 Kaiser, K. & Guggenberger, G. Sorptive stabilization of organic matter by microporous goethite: sorption into small pores vs. surface complexation. *European Journal of Soil Science* **58**, 45-59 (2007).

89 Ilani, T., Schulz, E. & Chefetz, B. Interactions of organic compounds with wastewater dissolved organic matter. *Journal of Environmental Quality* **34**, 552-562 (2005).

90 Niemeyer, J., Chen, Y. & Bollag, J.-M. Characterization of humic acids, composts, and peat by diffuse reflectance Fourier-transform infrared spectroscopy. *Soil Science Society of America Journal* **56**, 135-140 (1992).

91 Fu, H. & Quan, X. Complexes of fulvic acid on the surface of hematite, goethite, and akaganeite: FTIR observation. *Chemosphere* **63**, 403-410 (2006).

92 Fortin, D., Leppard, G. G. & Tessier, A. Characteristics of lacustrine diagenetic iron oxyhydroxides. *Geochimica et Cosmochimica Acta* **57**, 4391-4404 (1993).

93 Feyte, S., Tessier, A., Gobeil, C. & Cossa, D. In situ adsorption of mercury, methylmercury and other elements by iron oxyhydroxides and organic matter in lake sediments. *Applied Geochemistry* **25**, 984-995 (2010).

94 Chappaz, A., Gobeil, C. & Tessier, A. Geochemical and anthropogenic enrichments of Mo in sediments from perennially oxic and seasonally anoxic lakes in Eastern Canada. *Geochimica et Cosmochimica Acta* **72**, 170-184 (2008).

95 Laforte, L., Tessier, A., Gobeil, C. & Carignan, R. Thallium diagenesis in lacustrine sediments. *Geochimica et Cosmochimica Acta* **69**, 5295-5306 (2005).

96 Hanson, P. C., Pace, M. L., Carpenter, S. R., Cole, J. J. & Stanley, E. H. Integrating Landscape Carbon Cycling: Research Needs for Resolving Organic Carbon Budgets of Lakes. *Ecosystems* **18**, 363-375 (2015).

Appendix A: Sample preparation

This Appendix describes the details of both the reduction and control experiments described in the main text. Freeze dried, homogenized sediments were first subjected to a control experiment in order to remove any loosely bound OM targeted by the high ionic strength and temperature used in the DCB reduction method. The control experiment replaced all complexing reagents and electrochemically active species with NaCl in order to maintain the solutions ionic strength. The reduction itself was performed on the post control sediment samples. 0.11 M sodium bicarbonate and 0.27 M sodium citrate (total volume of 15 mL) were added in order to maintain circumneutral pH and as an iron complexing agent, respectively. The electrochemical reduction proceeds with the addition of 0.25 g sodium dithionite. The sodium citrate complexing agent was added in order to prevent re-adsorption of any solubilized Fe(II) to the remaining mineral matrix. The reduction itself was performed at 80 ºC for a total of 15 minutes. After centrifugation at 3000 g for 10 minutes the supernatant was removed and the solid phase was subjected to three times sea water rinses to remove any citrate remaining from the reduction method.

The solid phase was freeze-dried and homogenized in order to be analyzed by EA-IRMS and FT-IR, while the supernatant was acidified and filtered through a 0.7 μm GF/F filter for iron quantitation by ICP-MS. Figure A-1 shows the different steps was carried out for the control and reduction experiments.

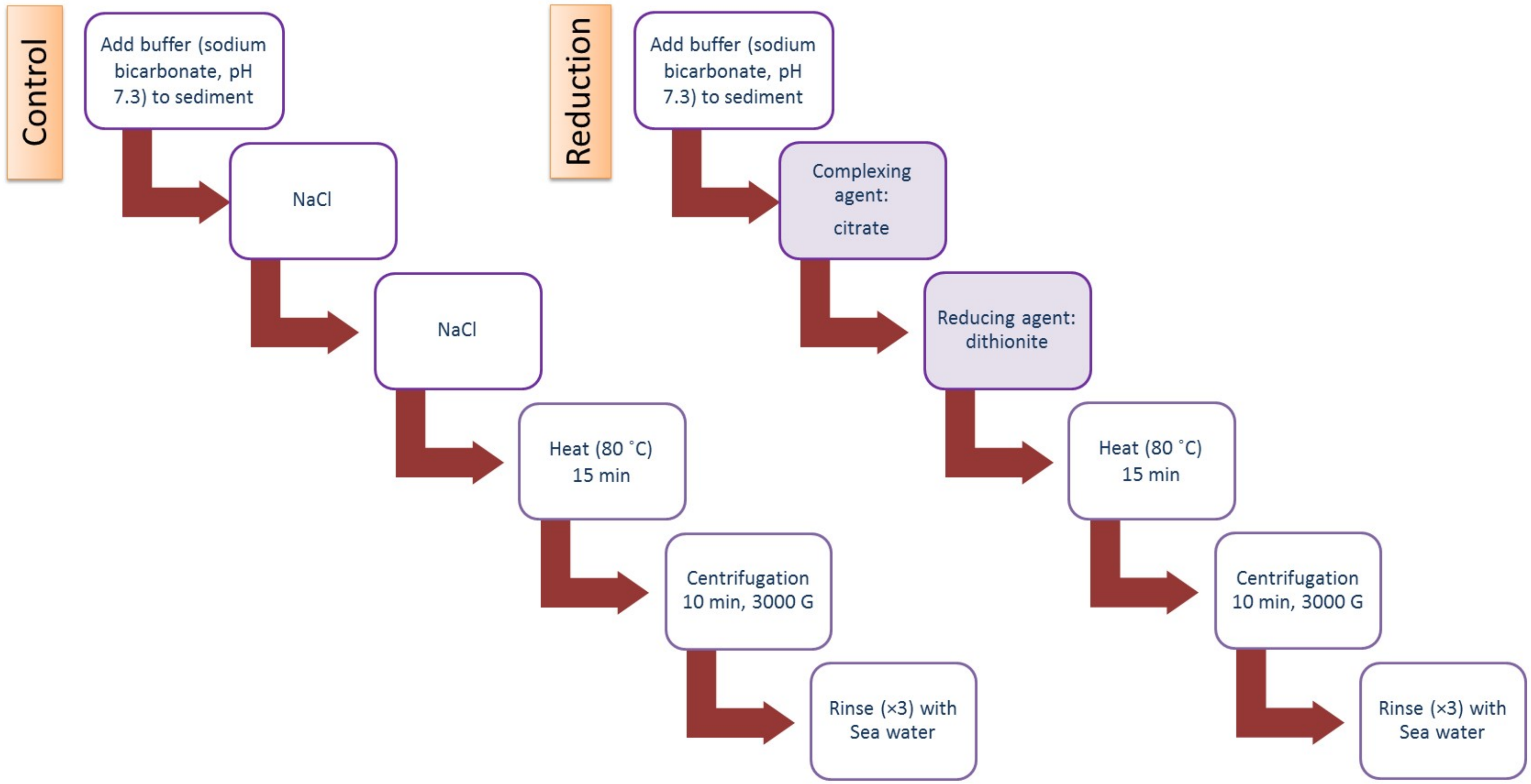

Figure A-1: The steps was carried out for the control and reduction experiment

Appendix B: FTIR spectra

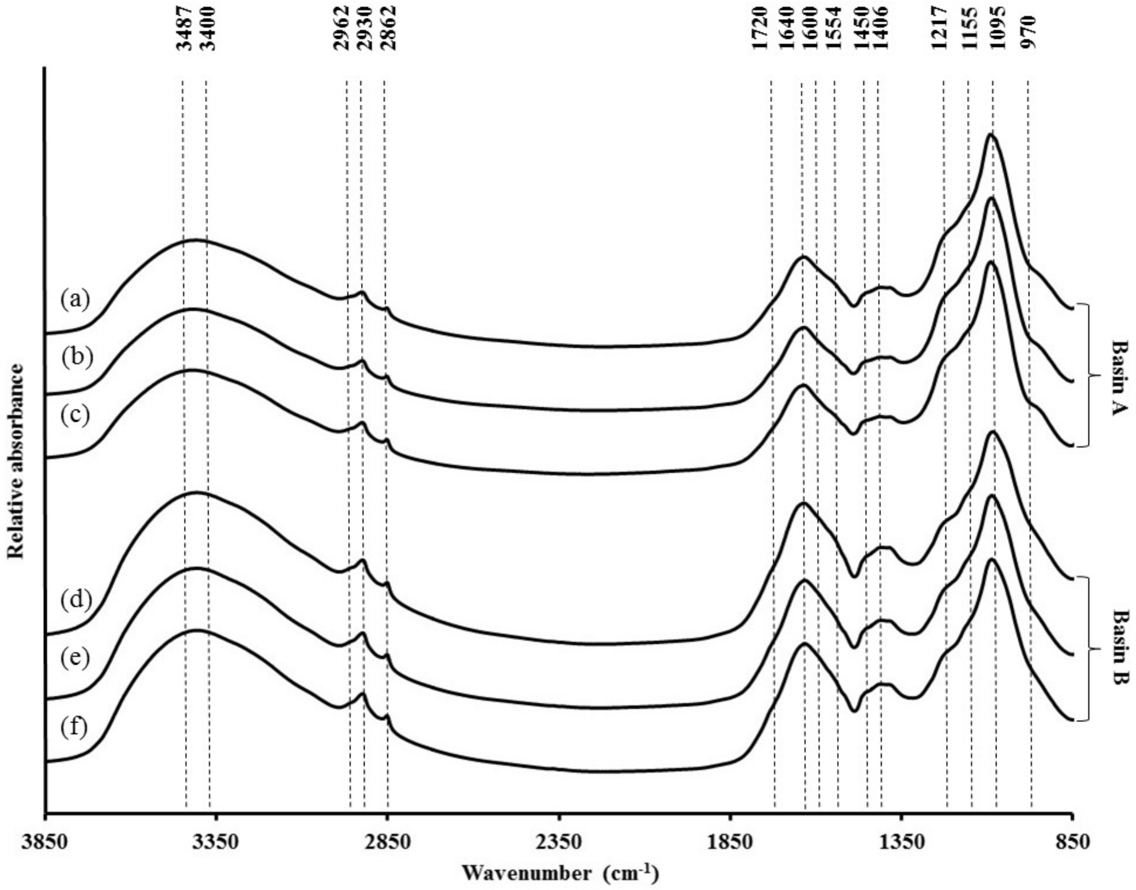

Figure B-1: FTIR spectra of the Initial OM at 1-2 cm (a and d), 8-9 cm (b and e) and 19-20 cm (c and f) of Basin A on top and Basin B at bottom.

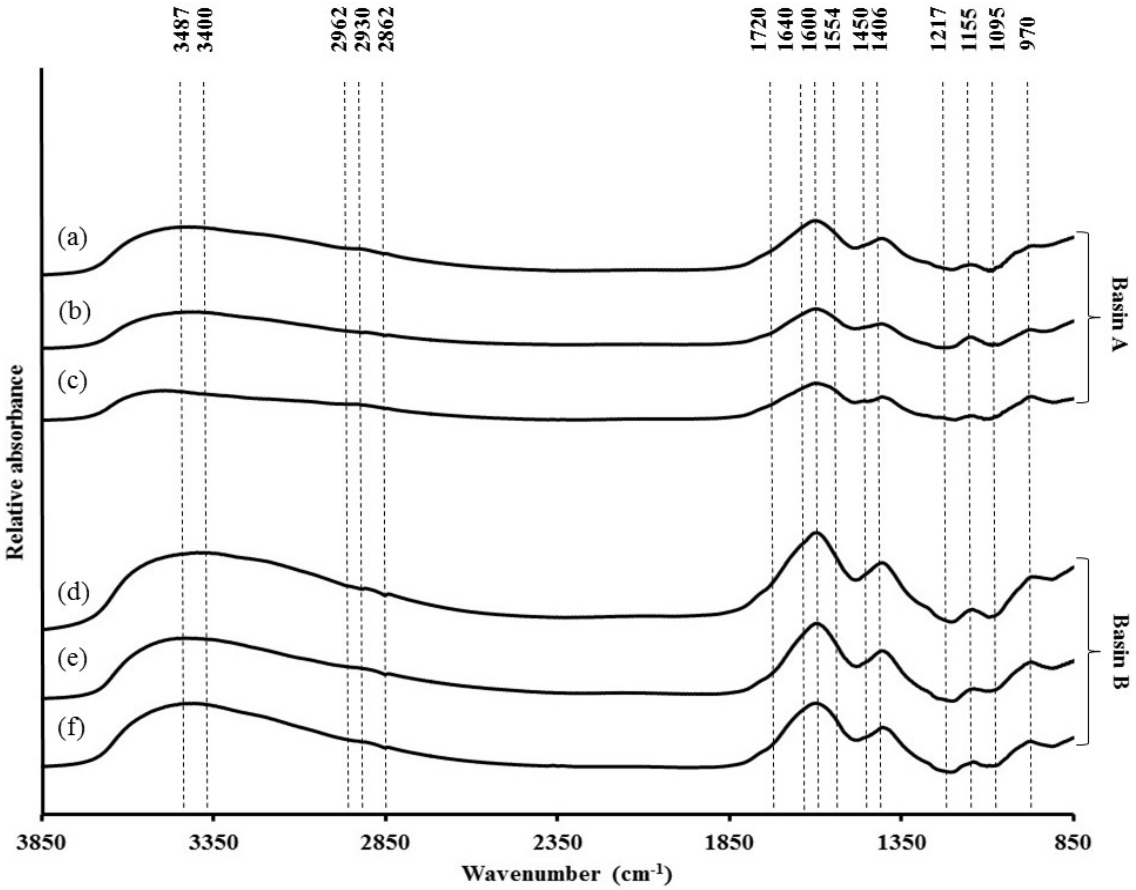

Figure B-2: FTIR spectra of the Fe-associated OM at 1-2 cm (a and d), 8-9 cm (b and e) and 19-20 cm (c and f) of Basin A on top and Basin B at bottom.

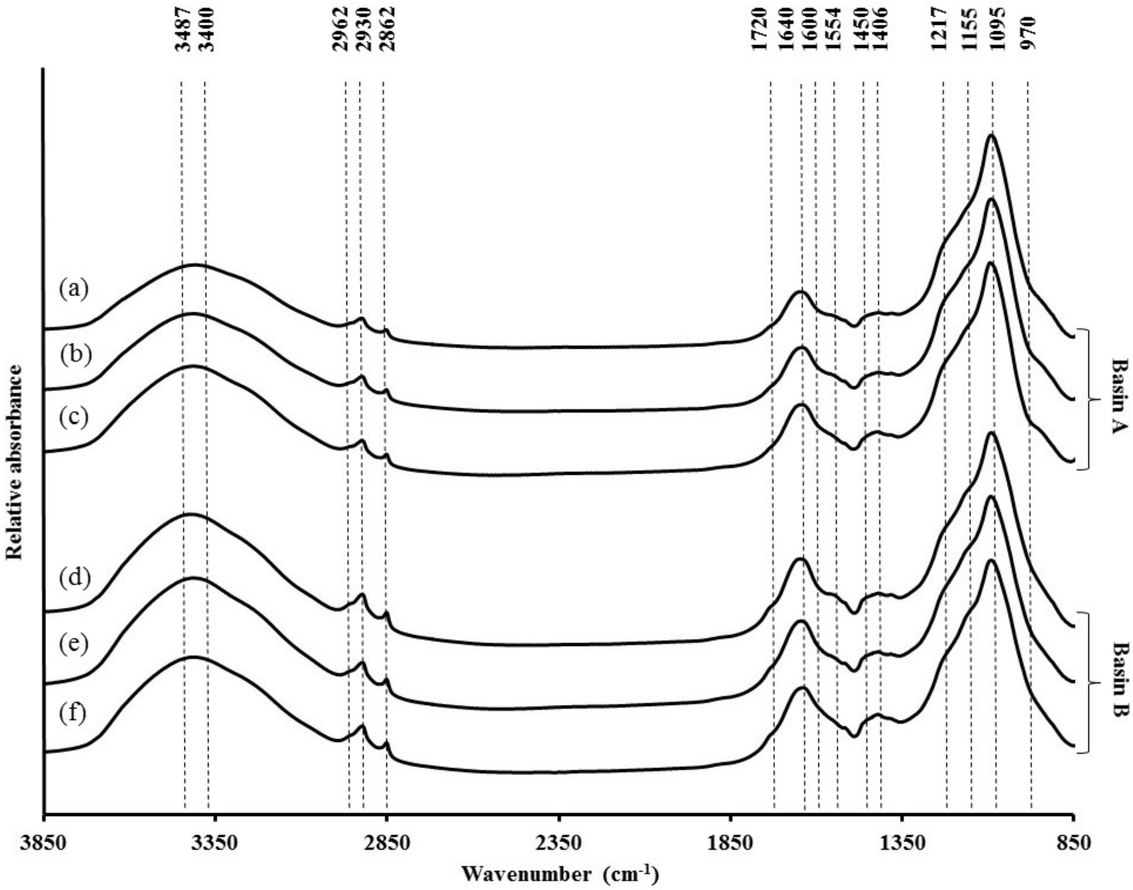

Figure B-3: FTIR spectra of the Residual at 1-2 cm (a and d), 8-9 cm (b and e) and 19-20 cm (c and f) of Basin A on top and Basin B at bottom.

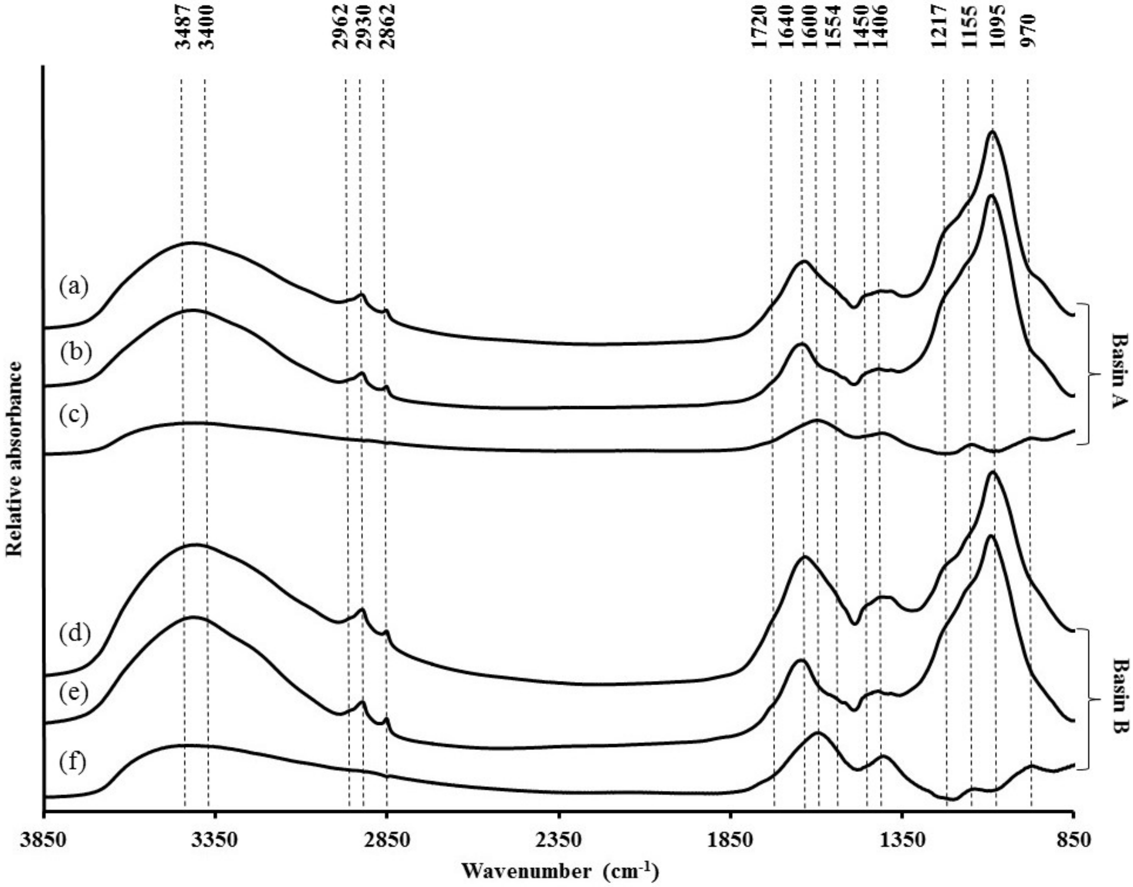

Figure B-4: FTIR spectra of the Initial (a and d), Residual (b and e) and Fe-associated (c and f) OM for sediment depth of 8-9 cm of Basin A on top and Basin B at bottom.

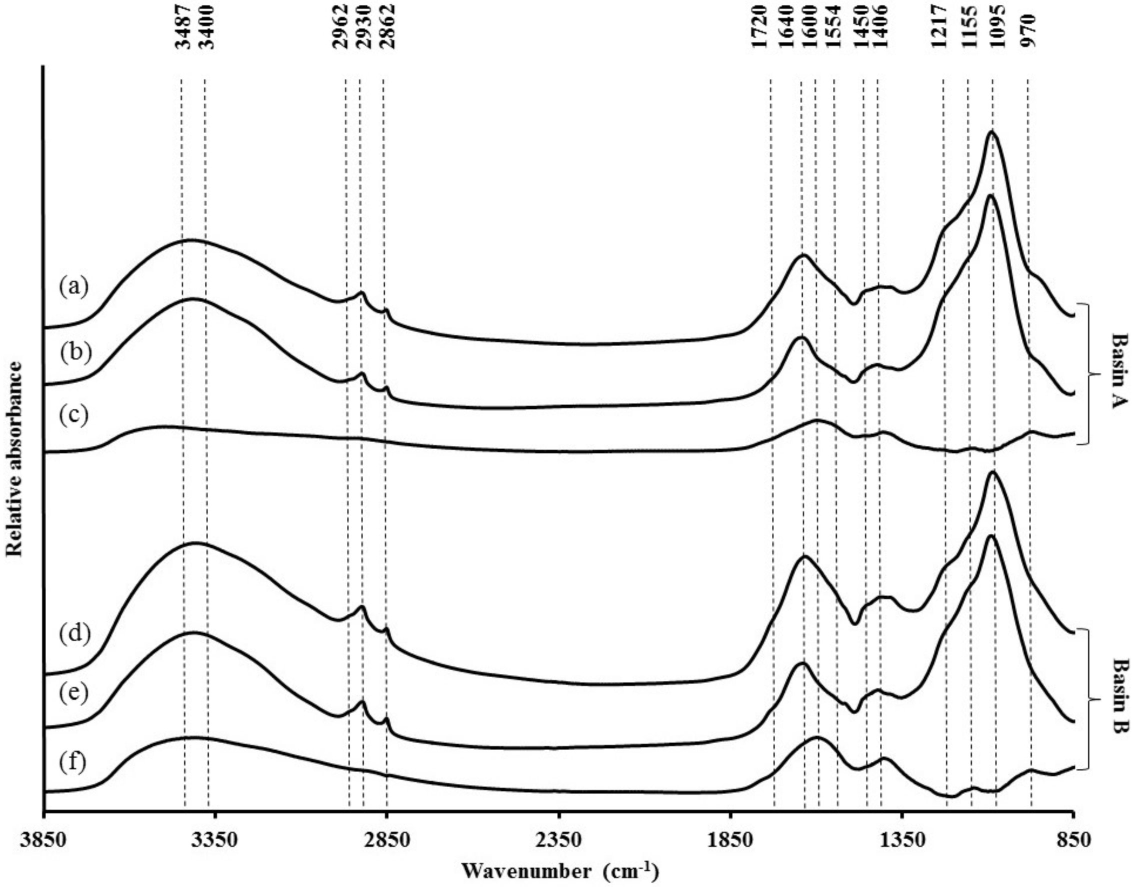

Figure B-5: FTIR spectra of the Initial (a and d), Residual (b and e) and Fe-associated (c and f) OM for sediment depth of 19-20 cm of Basin A on top and Basin B at bottom.